
Fairness Improves Learning from Noisily Labeled Long-Tailed Data

A PREPRINT

Jiaheng Wei
UC Santa Cruz

Zhaowei Zhu
UC Santa Cruz

Gang Niu
Riken

Tongliang Liu
University of Sydney

Sijia Liu
Michigan State University

Masashi Sugiyama
Riken & University of Tokyo

Yang Liu *
UC Santa Cruz & ByteDance Research

ABSTRACT

Both long-tailed and noisily labeled data frequently appear in real-world applications and impose significant challenges for learning. Most prior works treat either problem in an isolated way and do not explicitly consider the coupling effects of the two. Our empirical observation reveals that such solutions fail to consistently improve the learning when the dataset is long-tailed with label noise. Moreover, with the presence of label noise, existing methods do not observe universal improvements across different sub-populations; in other words, some sub-populations enjoyed the benefits of improved accuracy at the cost of hurting others. Based on these observations, we introduce the **Fairness Regularizer (FR)**, inspired by regularizing the performance gap between any two sub-populations. We show that the introduced fairness regularizer improves the performances of sub-populations on the tail and the overall learning performance. Extensive experiments demonstrate the effectiveness of the proposed solution when complemented with certain existing popular robust or class-balanced methods.

1 Introduction

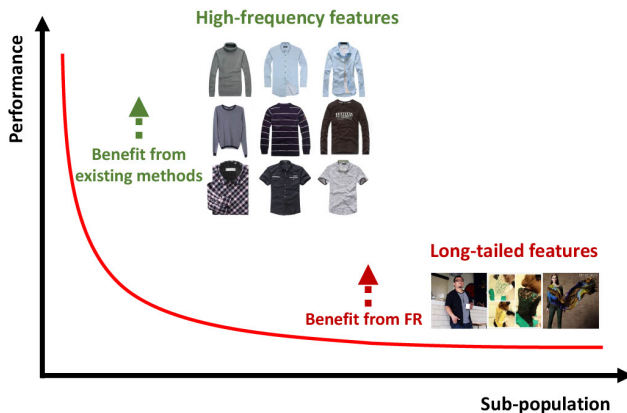


Figure 1: Overview of our work: Different robust solutions incur varied impacts on noisily labeled long-tailed distributed sub-populations. We show adding **Fairness Regularizer (FR)** between head and tail populations encourages the classifier to achieve relatively fair performances by reducing performance gaps among sub-populations, and improves the overall learning performance.

Biased and noisy training datasets are prevalent and impose challenges for learning [43, 70, 25]. The biases and noise can happen both at the sampling and label collection stages: A dataset often contains numerous sub-populations and

*Correspondence to yang.liu01@bytedance.com. (Paper under review)

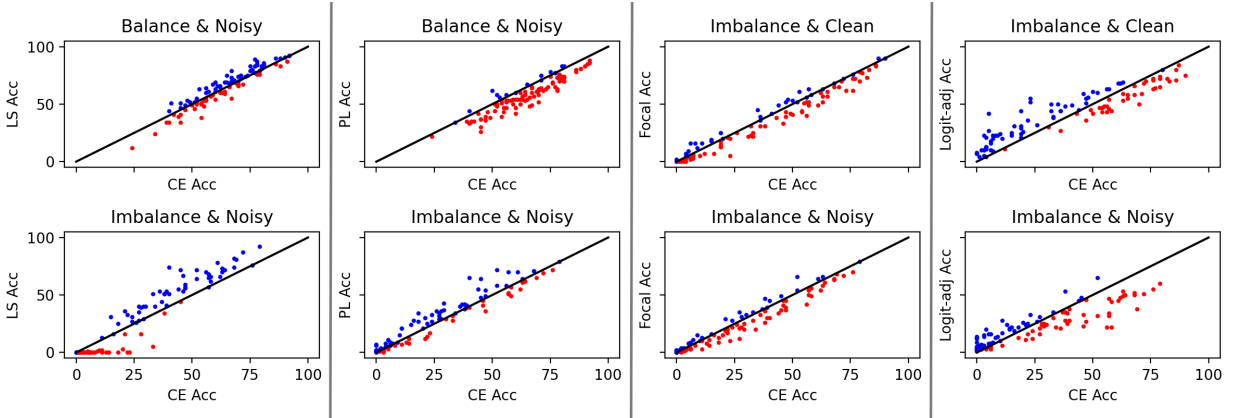


Figure 2: How each method improves per sub-population test accuracy w.r.t. CE loss on CIFAR-100 dataset. All methods are trained with Resnet-32. We treat the classes as a natural separation of sub-populations. For each sub-figure, the x -axis indicates the CE accuracy. y -axis denotes the performance of robust/long-tailed approaches. Each dot denotes the test accuracy pair $(\text{Acc}_{\text{CE}}, \text{Acc}_{\text{Method}})$ for each sub-population. The line $y = x$ stands for the case that CE performs the same as the robust treatment on a particular sub-population. The blue (red) dot above (below) the line shows the robust treatment has positive (negative) effect on this sub-population compared with CE. In the sub-titles, "Balance" denotes the balanced training data (w.r.t. clean labels); "Imbalance" means the training dataset follows a long-tailed distribution where the ratio between max and min number of samples in the sub-populations is 100; "Clean": the labels of training samples are clean; "Noisy": 20% correct labels are uniformly flipped into any other class. The test dataset is clean and balanced.

the size of these sub-populations tends to be long-tailed distributed [43, 70], where the tail sub-populations have an exponentially scaled probability of being under-sampled. Meanwhile, a dataset tends to suffer from noisy labels if collected from unverified sources [58]. Most prior works treat either population bias or label noise in an isolated way and do not explicitly consider the coupling effects of the two. In particular, existing works on learning with noisy labels mainly focus on a homogeneous treatment of the entire population, and the underlying clean data is often balanced [35, 24, 39, 26, 2].

The main inquiry of our paper is to understand and mitigate the possible heterogeneous effects of label noise when considering the imbalanced distribution of sub-populations. We start by presenting strong evidence of disparate impacts of sub-populations with a synthetic long-tailed noisy CIFAR-100 dataset [17] when using existing learning with noisy labels methods. Figure 2 illustrates the per-population (100 sub-populations in all, where we consider the class information as a natural separation of sub-populations) performance comparisons between applying the traditional Cross-Entropy (CE) loss and the recently proposed robust treatment to either noisy (i.e., Label Smoothing (LS) [27] and PeerLoss (PL) [26]) or long-tailed data (Focal [20], Logit-adjustment [33]). There are three main takeaways: *First*, the same robust treatment may have disparate impacts on different sub-populations, e.g., different sub-populations are improved differently by losses such as the Focal loss [20]. *Second*, different robust treatments have disparate impacts on the same part of data, e.g., LS [27] performs badly (almost 0 accuracies) on sub-populations with low CE accuracy (<50) and improves the others, while PL [26] has a reversed effect that the high CE accuracy part (>50) is likely to be degraded. *Third*, the prior works fail to address the coupling effects of population imbalance and noisy labels.

The above observations motivate us to explore how sub-population data should be treated when learning from noisily labeled long-tailed data. This work formally investigates the influence of sub-populations when learning with long-tailed and noisily labeled data. The analysis inspires us to define a fairness regularizer for this learning task. Figure 1 overviews our work. Our contributions are primarily two-fold. We quantify the influence of sub-populations using a number of metrics and discover disparate impacts of long-tailed sub-populations when label noise presents (Section 3). Following the above observation, we propose the **Fairness Regularizer (FR)**, which encourages the learned classifier to reduce the performance gap between the head and tail sub-populations. As a result, our approach not only improves the performances of tail populations but also improves overall learning performance. Extensive experiments on the CIFAR-10, CIFAR-100, and Clothing1M datasets demonstrate the effectiveness of **FR** when complemented with certain robust or long-tailed solutions (Section 5).

Contrary to most existing fairness-accuracy trade-offs observed in the literature [8, 34, 30, 68, 48, 10], we show that adding this fairness regularizer alleviates disparate impacts across populations of different sizes and improves the learning from noisily labeled long-tailed data.

1.1 Related Works

Learning with Noisy Labels Obtaining perfect annotations in supervised learning is a challenging task [65, 29, 58]. Due to the restrictions of human recognition, noisy annotations impose challenges to performing robust training. A line of popular approaches of learning with label noise firstly estimates the noise transition matrix, and then proceeds to use this knowledge to perform loss or sample correction [13, 35, 24, 39, 74, 19], i.e., the surrogate loss uses the transition matrix to define unbiased estimates of the true losses [45, 35, 44, 49, 31]. Noting that the estimation of the noise transition matrix is non-trivial [74, 75], another line of works aims to propose training methods without requiring knowing the noise rates, e.g., using robust loss functions [16, 26, 57, 55] training deep neural nets directly without the knowledge of noise rates [7, 52, 54, 40, 3], making use of the early stopping strategy [22, 62, 21, 23, 9], or designing a pipeline which dynamically selects/corrects and trains on "clean" samples with small loss [2, 63, 64, 14, 66]. Recent works also explored the possibility of using open-set data to improve the closed-set robustness [53, 61].

Learning with Long-Tailed Data The most relevant mainstream solution of learning with long-tailed clean data is the logit/loss adjustment approaches, which modify the loss values during the training procedure, for example, adjust the loss values w.r.t. the label frequency [41], sample influence [38], or the distribution alignment between model prediction and a set of the balanced validation set, among many other solutions. More recently, based on the label frequencies, the logit adjustments over classic approaches [32] are proposed, either through a post-hoc modification w.r.t. a trained model or enforcement in the loss during training. Open-set data may also be used to improve complement long-tailed data [53]. For interested readers, please refer to a comprehensive survey [67].

Existing robust approaches targeted mainly the class or sub-population level balanced training data. More recently, the literature observed several approaches to address the issue of label-noise in the long-tailed tasks, through decoupled treatments for head classes and tail ones, i.e., detecting noisy labels and performing robust solutions to the head class, meanwhile adopting a self/semi-supervised learning manner to deal with the tail classes [69, 60, 15]. Beyond classes, it has been demonstrated that sub-populations with different noise rates cause disparate impacts [25, 73] and need decoupled treatments [72, 50], which is more crucial for long-tailed sub-populations.

2 Preliminary

We go through the preliminaries in this section.

2.1 Sub-Populations of Features

In a K -class classification task, denote a set of data samples with clean labels as $S := \{(x_i, y_i)\}_{i=1}^n$, given by random variables (X, Y) , which is assumed to be drawn from \mathcal{D} . In this work, we are interested in how sub-populations intervene with learning. Formally, we denote $G \in \{1, 2, \dots, N\}$ as the random variable for the index of sub-population, and each sample (x_i, y_i) is further associated with a g_i . The set of sub-population k could then be denote as $\mathcal{G}_k := \{i : g_i = k\}$. We consider a long-tail scenario where the head population and the tail population differ significantly in their sizes, i.e., $\max_k |\mathcal{G}_k| \gg \min_{k'} |\mathcal{G}_{k'}|$.

Consider Figure 3 for an example of sub-population separations using the CIFAR-100 dataset [17]: images are grouped into 20 coarse classes, and each coarse class could be further categorized into 5 fine classes. For example, the coarse class "aquatic mammals" was further split into "beaver", "dolphin", "otter", "seal", and "whale". From Figure 3, we observe a strong imbalanced distribution of different sub-populations and a long-tailed pattern. In Section 5.1, we provide more details on long-tail data generation models for our synthetic experiments.

Clarification Throughout this work, the saying of sub-populations is a generalized definition of the separation of samples, which includes many popular settings as special cases, i.e.,

- *Class-relevant*: the class name is actually a natural separation of samples, such separations could be more fine-grained class-related (such as further splitting the class "cat" into finer separations by referring to the breed of cats);
- *Class-irrelevant*: such population could also be class-irrelevant, for example, in image classification tasks where the gender information is the (hidden) attribute information of each image while the class/label does not disclose this information.

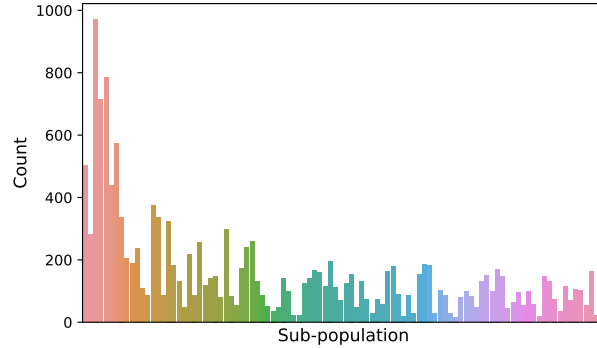


Figure 3: Count plot of a synthetic long-tailed CIFAR-100 train dataset: x -axis denotes the sub-population index; y -axis indicates the number of samples in each sub-population.

2.2 Our Task

In practice, obtaining "clean" labels from human annotators is both time-consuming and expensive. The obtained human-annotated labels usually consist of certain noisy labels [65, 18, 12, 58]. The flipping from clean labels to noisy labels is usually described by the noise transition matrix $T(X)$, with its element denoted by $T_{ij}(X) = \mathbb{P}(\tilde{Y} = j | Y = i, X)$. We denote the obtained noisy training dataset as $\tilde{S} := \{(x_i, \tilde{y}_i)\}_{i=1}^n$, given by random variables (X, \tilde{Y}) , which is assumed to be drawn from $\tilde{\mathcal{D}}$.

Though we only have access to noisily labeled long-tailed data \tilde{S} , our goal remains to obtain the optimal classifier with respect to a clean and balanced distribution \mathcal{D} : $\min_{f \in \mathcal{F}} \mathbb{E}_{(X, Y) \sim \mathcal{D}} [\ell(f(X), Y)]$, where f is the classifier chosen from the hypothesis space \mathcal{F} , and $\ell(\cdot)$ is a calibrated loss function (e.g., CE). Furthermore, we do not assume the knowledge of the sub-population information during training. We are interested in how sub-populations intervene with the learning performance and how we could improve by treating the sub-populations with special care.

3 Disparate Influences of Sub-Populations: An Empirical Study

In this section, we empirically illustrate the disparate influence of sub-populations when learning with noisily labeled data. Inspired by the literature on using the influence function to capture the impact of a subset of training data, we define influence metrics at the sub-population level and perform a multi-faceted evaluation of how the imbalanced sub-populations affect the learning performance. We take the long-tailed sub-populations for illustration and defer the results of head populations to Appendix C.4.

Influences: In the literature of explainable deep learning, the notions of influence can be different, e.g., the influences of features on an individual sample prediction [42, 47, 28, 5], the influences of features on the loss/accuracy of the model [37, 36], the influences of training samples on the loss/accuracy of the model [11]. In this section, we focus on the influence of a sub-population on both the sub-population level and the individual sample level.

We now empirically demonstrate the role of sub-populations when measuring the test accuracy, and the prediction of model confidence on test samples. For the synthetic long-tailed noisy training dataset, we first flip clean labels of the class-balanced CIFAR-10 dataset to any other classes, and there exist 20% wrong labels in all. We then adopt the class-imbalanced [4] CIFAR-10 dataset to select a long-tailed distributed amount of samples for each class (by referring to clean labels). As for the separation of sub-populations, we adopt the k -means clustering to categorize the extracted features of each feature given by the Image-Net pre-trained model. Since sub-population information sometimes may not be available for training use, understanding the influences of such division of sub-populations is beneficial. More separation details and experiment designs could be found at 5.1.

We explore the influences of tail sub-populations on performances of cross-entropy (ce) loss, the forward loss correction (fw) [39], label smoothing (ls) [27], and the peer loss (pl) [26]. There are 17 sub-populations (train) with less than 50 instances considered as the tail section.

We illustrate observations on several randomly selected tail sub-populations. Results of more sub-populations are deferred to Appendix C.1.

3.1 Influences on Sub-Population Level (Test Accuracy)

We start with the influence of sub-populations in the test set. We adopt the (population-level) test accuracy changes when removing all samples in the sub-population \mathcal{G}_i during the training procedure to capture the influences of a sub-population on each sub-population at the test set:

$$\text{Acc}_p(\mathcal{A}, \tilde{S}, i, j) = \mathbb{P}_{\substack{f \leftarrow \mathcal{A}(\tilde{S}) \\ (X', Y', G=j)}} (f(X') = Y') - \mathbb{P}_{\substack{f \leftarrow \mathcal{A}(\tilde{S} \setminus i) \\ (X', Y', G=j)}} (f(X') = Y'),$$

where in the above two quantities, $f \leftarrow \mathcal{A}(\tilde{S})$ indicates that the classifier f is trained from the whole noisy training dataset \tilde{S} via Algorithm \mathcal{A} , $f \leftarrow \mathcal{A}(\tilde{S} \setminus i)$ means f is trained on \tilde{S} without samples in the sub-population \mathcal{G}_i . $(X', Y', G = j)$ denotes the test data distribution given that the samples are from the j -th sub-population.

In Figure 4, the x -axis denotes the loss function for training, and the y -axis visualized the distribution of $\{\text{Acc}_p(\mathcal{A}, S, i, j)\}_{j \in [100]}$ (top) and $\{\text{Acc}_p(\mathcal{A}, \tilde{S}, i, j)\}_{j \in [100]}$ (bottom) for several long-tailed sub-populations ($i = 52, 70, 91$) under each robust method, where "S" refers to the clean training samples and " \tilde{S} " denotes the noisy version. The blue zone shows the 25-th percentile (Q_1) and 75-th percentile (Q_3) accuracy changes, and the orange line indicates the median value. Accuracy changes that are drawn as circles are viewed as outliers. Note that all sub-figures have the same limits for y -axis. It is clear to observe the top three figures have lower variance than the bottom ones, indicating that:

Observation 3.1. Compared with clean training, tail sub-populations in noisy training tend to have a more significant influence on the test accuracy.

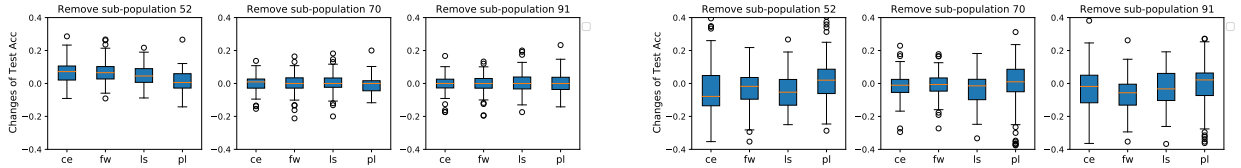


Figure 4: Box plot of the population-level test accuracy changes when removing all samples of a selected long-tailed sub-population during the training w.r.t. 4 methods. (Left: trained on clean labels; Right: trained on noisy labels.)

3.2 Influences on Sample Level (Prediction Confidence)

Note that grouping testing samples into classes/sub-populations for analysis may ignore some individual behavior changes, we next consider the influence of sub-populations on the individual test samples. Instead of insisting on the accuracy measure, we adopt the model prediction confidence as a proxy, to see how each test sample got influenced. And we introduce $\text{Infl}(\mathcal{A}, \tilde{S}, i, j)$ to quantify the influence of a sub-population on a specific test sample:

$$\text{Infl}(\mathcal{A}, \tilde{S}, i, j) = \mathbb{P}_{f \leftarrow \mathcal{A}(\tilde{S})} (f(x'_j) = y'_j) - \mathbb{P}_{f \leftarrow \mathcal{A}(\tilde{S} \setminus i)} (f(x'_j) = y'_j).$$

As shown in Figure 5, we visualize $\text{Infl}(\mathcal{A}, S, i, j)$ (Top) and $\text{Infl}(\mathcal{A}, \tilde{S}, i, j)$ (Bottom), where $j \in [10000]$ means 10K test samples. For example, $\text{Infl}(\mathcal{A}, \tilde{S}, i, j) = -1$ means the model prediction confidence on test sample x'_j changed from 0 to 1. With the presence of label noise, we observe:

Observation 3.2. Compared with clean training, removing certain tail sub-populations lead to significant changes/influences on the model prediction confidence of more test samples.

Concluding this section, we have shown that given certain robust methods, significant disparate impacts on sub-populations are observed, when learning from long-tailed data with noisy labels. Such impacts also differ when complemented with different robust solutions, i.e., robust loss functions implicitly incur disparate impacts on the populations/samples. Recall in Figure 2, we revealed that existing robust treatments may result in unfair performances among sub-populations, when learning from noisily labeled long-tailed data. All these observations motivate us to explore ways that will reduce the gaps between the head and the tail populations.

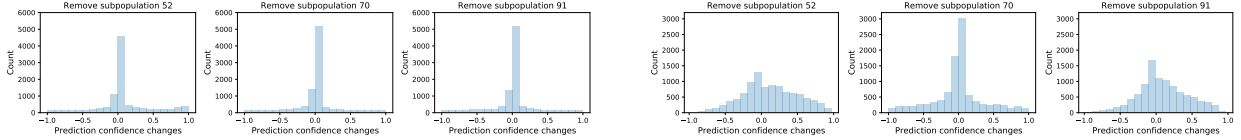


Figure 5: Distribution plot w.r.t. the changes of model confidence on the test data samples using CE loss (Left: trained on clean labels; Right: trained on noisy labels). See Appendix C.1 for more details. Removing population 91 appears to result in much worse model prediction confidence on test samples.

4 Fairness Regularizer (FR)

In this section, we propose to assign fairness constraints to the learning objective function. Leveraged into its Lagrangian form, such fairness constraints could be viewed as fairness regularizers that explicitly encourage the classifier to achieve fair performances among sub-populations. We name our solution the **Fairness Regularizer (FR)**, which encourages the learned classifier to achieve fair performance across sub-populations.

4.1 Fairness Constraints

Note that when learning with robust methods, the classifier tends to result in fitting on certain sub-populations more easily. We propose to constrain the classifier’s performance on sub-populations, i.e.,

$$\begin{aligned} & \min_{f: \text{domain}(X) \rightarrow [K]} \mathbb{E}_{(X, \tilde{Y}) \sim \tilde{\mathcal{D}}} [\ell(f(X), \tilde{Y})] \\ & \text{s.t. Constraint w.r.t. } \mathbb{P}(f(X) = \tilde{Y} \mid G = i), \end{aligned} \tag{1}$$

where ℓ is a generic loss function that could be any robust losses and the ultimate goal of the classifier f is categorizing the feature X into a specific class within $[K]$. Since we do not wish certain sub-populations to fall much behind others, i.e., in terms of accuracy, we constrain the performance gap between any two sub-populations by adopting the following constraint for Eqn. (1), specifically, for any sub-population $i \in [N]$, we require its performance to have a bounded distance from the average performance. Denote the distance (absolute performance gap) by

$$\text{Dist}_i := \left| \mathbb{P}(f(X) = \tilde{Y} \mid G = i) - \mathbb{P}(f(X) = \tilde{Y}) \right|,$$

then the optimization problem is formulated as:

$$\min_{f: X \rightarrow [K]} \mathbb{E}_{(X, \tilde{Y}) \sim \tilde{\mathcal{D}}} [\ell(f(X), \tilde{Y})], \quad \text{s.t. } \text{Dist}_i \leq \delta, \forall i \in [N], \tag{2}$$

where $\delta \geq 0$ is a constant. Setting $\delta = 0$ implies that the classifier should achieve fair performances among all sub-populations, in order to satisfy the constraints.

4.2 Using Fairness Constraints as a Regularizer

In practice, forcing sub-populations to achieve absolutely fair or equalized performances (i.e., accuracy) may produce side effects. For example, one trivial solution to achieve $\delta = 0$ is simply reducing the performance of all the other sub-populations to be aligned with the worst sub-population, leading to poor overall performance. Even though we can fine-tune δ to set an appropriate tolerance of the gap, the sub-population with the worst performance may still violate the constraint. Noting our goal is to improve the overall performance on clean and balanced test data, it is arguably a better strategy to not over-addressing the worst sub-population.

To balance the trade-off between mitigating the disparate impacts among sub-populations and the possible negative effect due to constraining, rather than strictly solving the constrained optimization problem in Eqn. (2), we use the constraint as a regularizer by converting it to its Lagrangian form as follows.

$$\min_{f: X \rightarrow [K]} \mathcal{L}_\lambda(f) := \mathbb{E}_{(X, \tilde{Y}) \sim \tilde{\mathcal{D}}} [\ell(f(X), \tilde{Y})] + \underbrace{\sum_{i=1}^N \lambda_i \text{Dist}_i}_{\text{FR}}$$

where $\lambda_i \geq 0$. Different from the traditional dual ascent of Lagrange multipliers [1], we fix λ_i during our training. Intuitively, applying dual ascent is likely to result in a large λ_i on the worst sub-population, inducing possible negative effects as we discussed above. Therefore, in such a minimization task, the accuracy/performance gaps between sub-populations are encouraged to be small and do not have to be exactly lower than any threshold.

Implementation Denote by $\mathbf{f}_x[\tilde{y}]$ the model’s prediction probability on the noisy label \tilde{y} given input x . Noting the probability in Dist_i is non-differentiable w.r.t f , we apply the following empirical relaxation [51]:

$$\text{Dist}_i := \left| \frac{\sum_{k=1}^N \mathbf{f}_{x_k}[\tilde{y}_k] \cdot \mathbb{1}(g_k = i)}{\sum_{k=1}^N \mathbb{1}(g_k = i)} - \frac{\sum_{k=1}^N \mathbf{f}_{x_k}[\tilde{y}_k]}{N} \right|, \quad (3)$$

where $\mathbb{1}(g_k = i) = 1$ when $g_k = i$ and 0 otherwise. For simplicity, we set all λ_i to a constant, i.e. $\lambda_i = \lambda$.

To demonstrate why **FR** helps with improving the learning from noisily labeled long-tailed data, we will provide extensive experiment studies in the next section. We have also adopted a binary Gaussian example and theoretically show:

Observation 4.1. When solving the risk minimization on the noisily labeled long-tailed data under the introduced fairness constraints returns the Bayes optimal classifier.

Due to space limits, we defer the detailed discussion to Appendix A.4.

5 Experiments

In this section, we verify the effectiveness of **FR** on the synthetic long-tailed noisy CIFAR datasets [17] and real-world large-scale noisily labeled long-tailed dataset CIFAR-10N [59], CIFAR-20N [59], CIFAR-100N [59], Animal-10N [46], and Clothing1M [65].

5.1 Experiment Designs on Synthetic Noisily Labeled Long-Tailed CIFAR Datasets

We empirically test the performance of **FR** on CIFAR-10 and CIFAR-100 datasets [17]. The original CIFAR-10 [17] dataset contains 60k 32×32 color images, 50k images for training, and 10k images for testing. The dataset is balanced and each image belongs to one of ten completely mutually exclusive classes. CIFAR-100 dataset shares the same statistics, except for containing 100 completely mutually exclusive classes.

Generation of Synthetic Long-Tailed Data with Noisy Labels Note that the class information could be viewed as a special case of sub-populations, in this subsection, we treat classes as the natural separation of sub-populations and consider the class-imbalance experiment setting with noisy labels. For the balanced K -class classification task with n samples per class, the synthetic long-tail setting assumes that k -th class has only $n/(r^{\frac{k-1}{K-1}})$ samples by referring to the ground-truth labels [4]. We adopt two label-noise transition models below.

Model 1 (Imb): The entries of the noise transition matrix are given by:

$$T_{i,j} := \mathbb{P}(\tilde{Y} = j | Y = i, X = x) = \begin{cases} 1 - \rho, & i = j, \\ \frac{\mathbb{P}(Y=j) \cdot \rho}{1 - \mathbb{P}(Y=i)}, & i \neq j, \end{cases}$$

where ρ is viewed as the overall error/noise rate. The Imb noise model [60] assumes that samples are more likely to be mislabeled as frequent ones in real-world situations.

Model 2 (Sym): The generation of the symmetric noisy dataset is adopted from [16], where it assumed that $T_{i,j} = \frac{\rho}{K-1}, \forall i \neq j$, indicating that any other classes $i \neq j$ has the same chance of being flipped to class j . The diagonal entry $T_{i,i}$ (chance of a correct label) becomes $1 - \rho$.

For both noise settings, we test **FR** with noise rates $\rho \in \{0.2, 0.5\}$, meaning the proportion of wrong labels in the long-tailed training set is 0.2 or 0.5.

Separation of \mathcal{G}_i For the experiments w.r.t. **FR**, we consider two kinds of sub-population separation methods.

- **Separation with Clustering Methods:** $\forall x \in X$, the representation of feature x is given by the representation extractor $\phi(x)$, where $\phi(\cdot) : X \rightarrow \mathbb{R}^d$ maps the feature x to a d -dimensional representation vector. Given a distance metric DM (i.e., the Euclidean distance), the distance between two extracted representations $\phi(x_1), \phi(x_2)$ is $\text{DM}(\phi(x_1), \phi(x_2))$. The sub-population could be separated through clustering algorithms such as k -means ($k = N$ here). Admittedly, obtaining a good representation extractor is non-trivial [71], we want to highlight that the separation of sub-populations is not highly demanding on the quality of the representation extractor, and the focus is to perform fairness regularizations on varied features.

Table 1: Performance comparisons on synthetic long-tailed noisy CIFAR datasets (noise type: imbalance-noise & symmetric noise), best-achieved test accuracy are reported. Results in **bold** (and green-colored) mean **FR** improves the performance of the baseline methods, respectively.

Noise type: Imbalance Noise												
Noise Ratio	CIFAR-10 ($\rho = 0.2$)			CIFAR-10 ($\rho = 0.5$)			CIFAR-100 ($\rho = 0.2$)			CIFAR-100 ($\rho = 0.5$)		
Imbalance Ratio	$r = 10$	$r = 50$	$r = 100$	$r = 10$	$r = 50$	$r = 100$	$r = 10$	$r = 50$	$r = 100$	$r = 10$	$r = 50$	$r = 100$
CE	79.75	65.98	60.03	65.38	47.51	37.44	46.02	31.44	26.98	29.58	16.93	13.87
CE + FR (KNN)	80.46	69.00	61.64	65.87	46.69	39.97	46.18	31.03	27.60	30.25	16.79	15.19
CE + FR (G2)	80.44	67.29	65.12	68.62	49.43	39.69	46.38	32.32	28.53	32.35	19.03	15.93
LS [27]	82.52	69.08	59.07	67.73	36.17	32.92	47.80	33.66	26.36	34.02	17.28	14.10
LS + FR (KNN)	82.78	70.06	59.27	68.99	36.55	36.63	48.27	33.01	27.60	32.01	17.14	14.07
LS + FR (G2)	82.02	70.24	60.33	70.50	44.11	35.49	47.30	33.86	29.67	34.51	17.84	16.68
NLS [56]	79.91	65.98	58.82	64.74	41.01	34.16	46.05	31.48	27.09	29.86	16.84	13.87
NLS + FR (KNN)	80.17	68.61	62.88	68.65	47.42	36.79	45.72	32.25	27.01	28.85	17.23	14.18
NLS + FR (G2)	80.36	68.25	63.50	69.70	49.01	38.26	43.15	33.78	28.69	32.30	19.62	15.64
Focal [20]	76.24	64.16	57.68	62.40	40.25	34.56	43.63	29.10	24.88	26.93	14.45	12.57
Focal + FR (KNN)	77.54	62.97	57.24	61.47	42.28	37.04	42.44	28.90	25.14	28.34	16.02	13.27
Focal + FR (G2)	78.56	66.07	56.55	64.10	43.61	38.15	45.63	31.87	27.58	29.80	17.67	15.30
PL [26]	78.43	55.61	54.20	47.71	31.96	30.13	45.32	33.05	29.91	28.01	20.25	16.65
PL + FR (KNN)	79.50	65.37	53.36	51.82	35.68	30.16	44.89	33.12	28.63	27.66	19.79	17.72
PL + FR (G2)	78.79	66.16	54.39	50.72	33.22	28.01	44.78	33.35	29.51	29.82	20.15	16.81
Logit-adj [33]	82.09	73.23	68.18	68.30	51.51	42.17	47.28	33.11	29.47	30.92	17.97	14.68
Logit-adj + FR (G2)	82.92	75.67	72.20	73.72	55.09	40.85	41.21	35.39	28.84	27.57	18.93	15.44
Logit-adj + FR (KNN)	82.48	73.65	68.48	70.89	49.23	42.93	47.66	33.18	29.50	31.85	17.59	15.25
Noise type: Symmetric Noise												
Noise Ratio	CIFAR-10 ($\rho = 0.2$)			CIFAR-10 ($\rho = 0.5$)			CIFAR-100 ($\rho = 0.2$)			CIFAR-100 ($\rho = 0.5$)		
Imbalance Ratio	$r = 10$	$r = 50$	$r = 100$	$r = 10$	$r = 50$	$r = 100$	$r = 10$	$r = 50$	$r = 100$	$r = 10$	$r = 50$	$r = 100$
CE	80.70	65.04	61.80	70.48	51.53	36.44	46.02	30.93	26.98	29.93	16.70	4.76
CE + FR (KNN)	81.19	69.95	63.97	71.75	52.93	45.63	46.33	30.82	27.19	31.12	17.68	15.39
CE + FR (G2)	81.64	70.84	65.14	71.44	56.50	46.33	47.70	34.34	30.78	31.58	21.70	19.10
LS [27]	83.23	71.69	65.69	72.85	50.59	30.98	47.90	33.81	29.95	26.56	21.74	19.39
LS + FR (KNN)	83.28	70.64	60.91	73.92	53.01	43.48	49.05	33.40	30.05	34.86	20.73	19.10
LS + FR (G2)	82.22	70.85	62.43	74.59	54.15	44.77	48.16	34.08	30.69	36.40	22.06	20.10
NLS [56]	80.79	66.22	61.47	70.11	50.57	36.55	46.11	31.14	27.32	30.51	17.16	5.18
NLS + FR (KNN)	81.08	69.29	63.58	70.27	54.86	36.50	48.20	35.03	28.29	28.87	19.10	6.65
NLS + FR (G2)	81.37	70.60	64.73	71.30	56.24	37.29	47.67	34.32	30.75	29.62	22.17	8.04
Focal [20]	77.77	61.54	56.02	67.20	43.12	38.20	35.93	23.23	21.84	27.31	16.18	14.71
Focal + FR (KNN)	78.03	64.57	56.77	67.87	41.89	36.34	42.79	30.17	25.08	28.22	16.37	14.50
Focal + FR (G2)	78.83	65.56	60.35	68.21	47.09	41.74	46.33	32.56	27.77	29.70	16.47	15.29
PL [26]	79.73	66.82	42.12	55.52	33.18	33.06	44.60	32.91	28.69	27.38	18.52	17.25
PL + FR (KNN)	79.42	64.91	58.80	53.86	38.41	32.71	45.60	32.32	28.34	27.63	18.86	16.48
PL + FR (G2)	79.37	66.71	58.98	55.68	38.08	33.52	46.83	33.17	29.67	28.12	19.48	17.62
Logit-adj [33]	80.50	62.42	50.28	60.38	32.45	27.32	46.50	29.24	23.80	28.79	12.65	9.22
Logit-adj + FR (KNN)	80.66	62.07	51.04	62.32	31.23	22.41	47.22	29.34	24.70	29.95	12.44	9.28
Logit-adj + FR (G2)	81.82	62.62	52.35	63.34	31.14	21.93	48.13	30.18	24.06	29.35	12.37	9.26

- **Separation Directly via Pre-Trained Models:** In this case, $\forall x \in X$, we adopt an (Image-Net) pre-trained model for the separation, i.e., such a feature extractor $\phi(\cdot)$ maps each x into a $d = N$ -dimensional representation vector so that all features are automatically categorized into N sub-populations.

5.2 Experiment Results on Synthetic Noisily Labeled Long-Tailed CIFAR Datasets

In Table 1, we empirically show how **FR** helps with improving the classifier’s performance when complemented with several methods in robust losses as well as approaches in class-imbalanced learning, under synthetic class-imbalanced CIFAR datasets with noisy labels, including Cross-Entropy loss (CE), Label Smoothing (LS) [27], Negative Label Smoothing (NLS) [56], Focal Loss [20], PeerLoss (PL) [26], and Logit-adjustment (Logit-adj) [33]. We fix the same training samples and labels for all methods. More details are available in Appendix C.2.

For **FR**, we adopted the fixed λ for all sub-populations. We consider two types of sub-population separation methods: (i) KNN clustering, which splits the extracted features into K clusters, with K being the number of classes; (ii) Generate the separation by referring to the direct prediction made by an (Image-Net) pre-trained model. In our experiments, this method separates features into a head and a tail sub-population, and the ratio w.r.t. the amount of samples between two sub-populations is usually close to 5.

Results In Table 1, we provide the baseline performance as well as the corresponding performances when **FR** is introduced. **FR** (KNN) denotes the scenario where we adopt the KNN clustering for sub-population separation, and the number of sub-populations is the same as the number of classes. We did not consider the noisy (class) labels as the sub-population index due to the fact that the noisy labels may contain the wrong ones. Empirically, we observe that **FR** (KNN) consistently improves the baseline methods on the class-imbalanced CIFAR-10 dataset, under the Imb and Sym noise. However, **FR** (KNN) could not improve significantly on the class-imbalanced CIFAR-100 dataset. One reason is that, in the batch update, the number of samples in each sub-population is too small (the average number is $128/100 = 1.28$), resulting in large variance in calculating **FR** as Eqn. (3). As an alternative, we report the performance of **FR** (G2) as well, where samples are categorized into 2 sub-populations by the (Image-Net) pre-trained model. Surprisingly, **FR** (G2) improves the performance of 6 baselines in most settings, as highlighted in Table 1. Thus, constraining the classifier to have relatively fair performances improves learning from noisy and long-tailed data.

We further adopt the CIFAR-10 dataset ($\rho = 0.5, r = 50$) and visualize how **FR** influences the per-class accuracy by referring to the performance of each baseline. Each blue point in Figure 6 indicates the scenario where **FR** improves the test accuracy of a class over the corresponding baseline. Points in the lower left corner (where tail populations are usually located) further illustrate that **FR** consistently improves the performance of tail sub-populations.

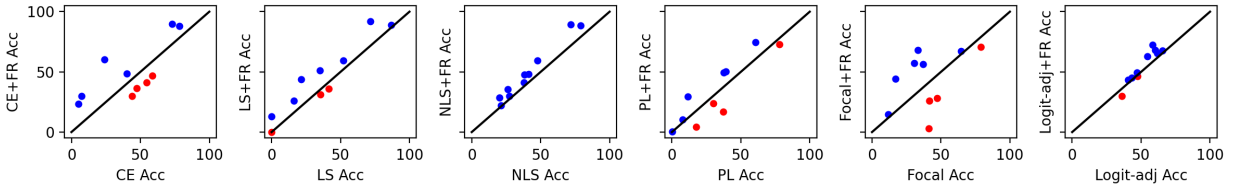


Figure 6: How **FR** improves per class test accuracy w.r.t. the baseline method on CIFAR-10. In each sub-figure, the x -axis indicates the accuracy of a baseline. y -axis denotes the performance of baseline when **FR** is introduced. Each dot denotes the test accuracy pair $(\text{Acc}_{\text{Method}}, \text{Acc}_{\text{Method+FR}})$ for each sub-population. The black line $y = x$ stands for the case that **FR** has no effects on a particular sub-population. The blue (red) dot above (below) the line shows the robust treatment has positive (negative) effect on this sub-population compared with CE.

We next adopt hypothesis testing to demonstrate the effectiveness of **FR**.

Hypothesis Testing w.r.t. FR We adopt paired student t-test to verify the conclusion that **FR** helps with improving the test accuracy. Briefly speaking, for each dataset and each baseline method, we statistically test whether **FR** results in significant test accuracy improvements in Table 1.

Denote by $\text{PA}_{\text{Method}}^{\rho,r} := (\text{Acc}_{\text{Method}}^{\rho,r}, \text{Acc}_{\text{Method+FR}}^{\rho,r})$ the Paired Accuracies without/with **FR** under each setting, i.e., when $\rho = 0.2, r = 10, \text{Method}=\text{CE}$, we have: $\text{PA}_{\text{Method}}^{\rho,r} = (79.75, 80.46)$ (w.r.t. **FR** (KNN)). The null and alternative hypotheses could be expressed as:

$$\begin{aligned} \mathbf{H}_0 &: \{\text{Acc}_{\text{Method+FR}}^{\rho,r}\}_{\rho,r} \text{ come from the same distribution as } \{\text{Acc}_{\text{Method}}^{\rho,r}\}_{\rho,r}; \\ \mathbf{H}_1 &: \{\text{Acc}_{\text{Method+FR}}^{\rho,r}\}_{\rho,r} \text{ come from different distributions as } \{\text{Acc}_{\text{Method}}^{\rho,r}\}_{\rho,r}, \end{aligned}$$

where the above accuracy list $\{\text{Acc}_{\text{Method}}^{\rho,r}\}_{\rho,r}$ includes both noise types (imb & sym), $\rho \in [0.2, 0.5]$, and $r \in [10, 50, 100]$, thus 12 elements for either dataset, similarly for the accuracy list $\{\text{Acc}_{\text{Method+FR}}^{\rho,r}\}_{\rho,r}$.

In Table 2, positive statistics indicate that the **FR** generally improves the performance (test accuracy) of the baseline method. The p -value that is smaller than 0.1 means there exist significant differences between the two accuracy lists. In such scenarios, we should reject the null hypothesis and adopt the alternative hypothesis. Table 2 shows that **FR** (G2) brings significant performance improvements in most settings (5/6 in CIFAR-10 and 6/6 in CIFAR-100), indicating the effectiveness of our method. Besides, **FR** (KNN) shows significant performance improvements only in several settings (but there are still improvements in most cases), which can be explained by our previous discussion that a large number of sub-populations may make the learning unstable. More details appear in Appendix C.2.

5.3 Experiments on Long-Tailed Data with Real-World Noisy Labels

We further provide more experiment results on real-world noisily labeled long-tailed data, including long-tailed CIFAR-10N, CIFAR-20N, CIFAR-100N, and Animal-10N.

Dataset Statistics Denote by ρ the percentage of wrong labels among the training set, CIFAR-10N [59] provides three types of real-world noisy human annotations on the CIFAR-10 training dataset, with $\rho = 0.09, 0.18, 0.40$. CIFAR-

Table 2: Paired student t-test results w.r.t. the effectiveness of **FR**. Rows marked with " \checkmark " mean **FR** improve the performance of the baseline methods significantly (p -value satisfies that $p < 0.1$ and the statistics is positive); "-" indicates there exist no significant differences after adopting **FR**.

Method	FR Type	CIFAR-10			CIFAR-100		
		statistics	p -value	Better	statistics	p -value	Better
CE	FR (KNN)	2.962	0.013	\checkmark	1.489	0.165	-
CE	FR (G2)	4.313	0.001	\checkmark	3.083	0.010	\checkmark
LS	FR (KNN)	1.214	0.250	-	0.748	0.470	-
LS	FR (G2)	1.851	0.091	\checkmark	1.926	0.080	\checkmark
NLS	FR (KNN)	4.235	0.001	\checkmark	1.692	0.119	-
NLS	FR (G2)	4.909	<0.000	\checkmark	3.237	0.008	\checkmark
PL	FR (KNN)	1.859	0.090	\checkmark	-0.620	0.548	-
PL	FR (G2)	1.847	0.092	\checkmark	2.345	0.039	\checkmark
Focal	FR (KNN)	0.886	0.395	-	2.218	0.049	\checkmark
Focal	FR (G2)	5.249	<0.000	\checkmark	4.105	0.002	\checkmark
Logit-adj	FR (KNN)	1.171	0.266	-	-0.419	0.684	-
Logit-adj	FR (G2)	0.255	0.803	-	2.410	0.035	\checkmark

100N [59] provides each CIFAR-100 training image with a human annotation where $\rho = 0.40$. In CIFAR-20N [59] ($\rho = 0.25$), each training/test image includes a coarse label (among 20 coarse classes) and a finer label (among 100 fine classes). We view the coarse label as the class information for training, and we illustrate the effectiveness of all methods by referring to their averaged performance on 100 sub-populations at the test time. Neither the number of sub-population nor the sub-population information of each image is utilized during the training. Animal-10N [46] dataset is a ten classes classification task including 5 pairs of confusing animals with a total of 55,000 images. The simulation of long-tailed samples follows the same procedure as the results in Table 1.

Hyperparameters The training of CIFAR-10N, CIFAR-20N, and CIFAR-100N is the same as that of synthetic noisy CIFAR datasets. For Animal10N, we adopt VGG19, a different backbone from ResNet. In Animal10N, the settings follow the work [46]: we use VGG-19 with batch normalization and the SGD optimizer. The network trained 100 epochs and we adopted an initial learning rate of 0.1, which is divided by 5 at 50% and 75% of the total number of epochs.

Results As shown in the three tables below, we report the test accuracy on the class-balanced dataset with clean labels, as we have done in Table 1 of the main paper. We adopt $\lambda = 2$ for CE+FR for all settings and $\lambda = 1$ for Logit-adj loss for all settings. Experiment results show that FR helps with improving the test accuracy in most settings, given CE loss or logit-adj loss. And we can conclude that constraining the classifier to have relative fairness performances is beneficial when learning with noisy and long-tailed data.

Table 3: Performance comparisons on long-tailed data with real-world noisy datasets. Best-achieved test accuracies are reported. Results in **bold** (and green-colored) mean **FR** improves the performance of the baseline methods, respectively.

Noise type: Real-World Human Noise						
Imbalance Ratio ($r = 10$)	CIFAR-10N (Agg)	CIFAR-10N (Rand1)	CIFAR-10N (Worse)	CIFAR-100N	CIFAR-20N	Animal-10N
CE	83.60	81.53	71.83	43.10	60.08	71.18
CE + FR (G2)	83.69	81.86	74.67	44.79	61.24	72.04
Logit-adj [33]	84.03	78.85	64.41	41.93	58.98	67.78
Logit-adj + FR (G2)	84.88	80.37	65.15	43.48	59.89	69.64
Imbalance Ratio ($r = 50$)	CIFAR-10N (Agg)	CIFAR-10N (Rand1)	CIFAR-10N (Worse)	CIFAR-100N	CIFAR-20N	Animal-10N
CE	74.54	71.55	61.36	32.51	50.83	52.60
CE + FR (G2)	74.93	73.22	65.01	34.49	51.93	51.88
Logit-adj [33]	75.67	66.15	52.93	30.06	46.83	56.28
Logit-adj + FR (G2)	75.81	65.94	54.36	30.47	47.00	62.18
Imbalance Ratio ($r = 100$)	CIFAR-10N (Agg)	CIFAR-10N (Rand1)	CIFAR-10N (Worse)	CIFAR-100N	CIFAR-20N	Animal-10N
CE	69.09	64.58	57.40	29.04	45.64	42.64
CE + FR (G2)	69.75	66.43	59.14	31.97	46.70	45.28
Logit-adj [33]	71.35	61.96	47.86	26.91	40.80	13.06
Logit-adj + FR (G2)	70.39	59.19	47.48	28.12	41.09	48.30

Table 4: Performance comparisons on real-world imbalanced noisily labeled dataset (Clothing1M), best and last-epoch achieved test accuracy are reported. Results in **bold** mean **FR** improves the performance of the baseline methods, respectively. Performances of **FR** with different λ s are provided.

Method	λ	0.0	0.1	0.2	0.4	0.6	0.8	1.0	2.0
CE	Best	72.68	72.44	72.93	72.74	73.10	72.80	72.99	72.45
	Last	72.22	71.99	72.25	72.24	72.51	72.53	72.58	72.20
LS	Best	72.55	72.71	72.69	72.34	72.41	72.44	72.70	72.56
	Last	72.03	72.11	72.14	72.12	72.12	72.06	72.33	72.24
NLS	Best	74.46	74.48	74.47	74.49	74.48	74.49	74.49	74.50
	Last	74.00	73.99	73.97	73.98	73.98	73.97	73.97	73.97
PL	Best	73.00	73.27	73.13	73.15	73.13	73.22	73.08	73.02
	Last	72.73	72.91	72.87	72.69	72.76	73.12	72.71	72.69
Focal	Best	72.71	72.60	72.71	72.60	72.92	72.66	72.91	72.46
	Last	72.16	72.21	72.04	72.18	72.30	72.36	72.51	72.46
Logit-adj	Best	72.43	72.52	72.48	71.88	72.22	72.45	72.67	72.06
	Last	72.22	72.15	72.14	71.58	71.83	71.94	72.23	71.92

5.4 Experiment Results on Clothing1M Dataset

Clothing1M is a large-scale feature-dependent human-level noisy clothes dataset. We adopt the same baselines as reported in CIFAR experiments for Clothing1M. Due to space limits, we defer detailed descriptions into Appendix C.3.

We try implementing **FR** with different λ chosen from the set $\{0.0, 0.1, 0.2, 0.4, 0.6, 0.8, 1.0, 2.0\}$, where $\lambda = 0.0$ indicates the training of baseline methods without **FR**. In Table 4, the default setting of **FR** ($\lambda = 1.0$) consistently reaches competitive performances by comparing to other λ s, except for the experiments w.r.t. NLS. Besides, we observe that most positive λ s that are close to $\lambda = 1.0$ tend to have better performances than those close to $\lambda = 0.0$, indicating the effectiveness as well as hyper-parameter in-sensitiveness of the introduced fairness regularizer.

6 Conclusions

In this paper, we qualitatively and quantitatively analyzed the influence of sub-populations under various metrics, where we observed disparate impacts incurred by sub-populations, especially when the label noise presents. What is more, our experiment results also reveal that existing robust solutions improve the performance of certain sub-populations at the cost of hurting others, hence leading to unfair performances among sub-populations. We then propose **Fairness Regularizer (FR)**, which encourages the learned classifier to achieve fair performances across sub-populations. Extensive experiment results demonstrate the effectiveness of **FR**, indicating that fairness constraints improve the learning from noisily labeled long-tailed data.

Acknowledgement

This work is partially supported by the National Science Foundation (NSF) under grants IIS-2007951, IIS-2143895, and IIS-2040800 (FAI program in collaboration with Amazon).

References

- [1] Stephen Boyd, Neal Parikh, Eric Chu, Borja Peleato, Jonathan Eckstein, et al. Distributed optimization and statistical learning via the alternating direction method of multipliers. *Foundations and Trends® in Machine learning*, 3(1):1–122, 2011.
- [2] Hao Cheng, Zhaowei Zhu, Xingyu Li, Yifei Gong, Xing Sun, and Yang Liu. Learning with instance-dependent label noise: A sample sieve approach. In *International Conference on Learning Representations*, 2021.
- [3] Hao Cheng, Zhaowei Zhu, Xing Sun, and Yang Liu. Mitigating memorization of noisy labels via regularization between representations. In *International Conference on Learning Representations*, 2023.
- [4] Yin Cui, Menglin Jia, Tsung-Yi Lin, Yang Song, and Serge Belongie. Class-balanced loss based on effective number of samples. In *Proceedings of the IEEE/CVF conference on computer vision and pattern recognition*, pages 9268–9277, 2019.
- [5] Vitaly Feldman and Chiyuan Zhang. What neural networks memorize and why: Discovering the long tail via influence estimation. *arXiv preprint arXiv:2008.03703*, 2020.
- [6] Priya Goyal, Piotr Dollár, Ross Girshick, Pieter Noordhuis, Lukasz Wesolowski, Aapo Kyrola, Andrew Tulloch, Yangqing Jia, and Kaiming He. Accurate, large minibatch sgd: Training imagenet in 1 hour. *arXiv preprint arXiv:1706.02677*, 2017.
- [7] Bo Han, Quanming Yao, Xingrui Yu, Gang Niu, Miao Xu, Weihua Hu, Ivor Tsang, and Masashi Sugiyama. Co-teaching: Robust training of deep neural networks with extremely noisy labels. In *Advances in neural information processing systems*, pages 8527–8537, 2018.
- [8] Moritz Hardt, Eric Price, and Nati Srebro. Equality of opportunity in supervised learning. *Advances in neural information processing systems*, 29, 2016.
- [9] Huaxi Huang, Hui Kang, Sheng Liu, Olivier Salvado, Thierry Rakotoarivelo, Dadong Wang, and Tongliang Liu. Paddles: Phase-amplitude spectrum disentangled early stopping for learning with noisy labels. *arXiv preprint arXiv:2212.03462*, 2022.
- [10] Rashidul Islam, Shimei Pan, and James R Foulds. Can we obtain fairness for free? In *Proceedings of the 2021 AAAI/ACM Conference on AI, Ethics, and Society*, pages 586–596, 2021.
- [11] Ruoxi Jia, David Dao, Boxin Wang, Frances Ann Hubis, Nick Hynes, Nezihe Merve Gürel, Bo Li, Ce Zhang, Dawn Song, and Costas J Spanos. Towards efficient data valuation based on the shapley value. In *The 22nd International Conference on Artificial Intelligence and Statistics*, pages 1167–1176. PMLR, 2019.
- [12] Lu Jiang, Di Huang, Mason Liu, and Weilong Yang. Beyond synthetic noise: Deep learning on controlled noisy labels. In *International Conference on Machine Learning*, pages 4804–4815. PMLR, 2020.
- [13] Zhimeng Jiang, Kaixiong Zhou, Zirui Liu, Li Li, Rui Chen, Soo-Hyun Choi, and Xia Hu. An information fusion approach to learning with instance-dependent label noise. In *International Conference on Learning Representations*, 2021.
- [14] Zhimeng Jiang, Kaixiong Zhou, Zirui Liu, Li Li, Rui Chen, Soo-Hyun Choi, and Xia Hu. An information fusion approach to learning with instance-dependent label noise. In *International Conference on Learning Representations*, 2022.
- [15] Shyamgopal Karthik, Jérôme Revaud, and Chidlovskii Boris. Learning from long-tailed data with noisy labels. *arXiv preprint arXiv:2108.11096*, 2021.
- [16] Youngdong Kim, Junho Yim, Juseung Yun, and Junmo Kim. Nlnl: Negative learning for noisy labels. In *Proceedings of the IEEE/CVF International Conference on Computer Vision*, pages 101–110, 2019.
- [17] Alex Krizhevsky, Geoffrey Hinton, et al. Learning multiple layers of features from tiny images. 2009.
- [18] Kuang-Huei Lee, Xiaodong He, Lei Zhang, and Linjun Yang. Cleannet: Transfer learning for scalable image classifier training with label noise. In *Proceedings of the IEEE Conference on Computer Vision and Pattern Recognition*, pages 5447–5456, 2018.
- [19] Shikun Li, Xiaobo Xia, Hansong Zhang, Yibing Zhan, Shiming Ge, and Tongliang Liu. Estimating noise transition matrix with label correlations for noisy multi-label learning. In *Advances in Neural Information Processing Systems*, 2022.
- [20] Tsung-Yi Lin, Priya Goyal, Ross Girshick, Kaiming He, and Piotr Dollár. Focal loss for dense object detection. In *Proceedings of the IEEE international conference on computer vision*, pages 2980–2988, 2017.

- [21] Sheng Liu, Kangning Liu, Weicheng Zhu, Yiqiu Shen, and Carlos Fernandez-Granda. Adaptive early-learning correction for segmentation from noisy annotations. In *Proceedings of the IEEE/CVF Conference on Computer Vision and Pattern Recognition*, pages 2606–2616, 2022.
- [22] Sheng Liu, Jonathan Niles-Weed, Narges Razavian, and Carlos Fernandez-Granda. Early-learning regularization prevents memorization of noisy labels. *Advances in neural information processing systems*, 33:20331–20342, 2020.
- [23] Sheng Liu, Zhihui Zhu, Qing Qu, and Chong You. Robust training under label noise by over-parameterization. In *International Conference on Machine Learning*, pages 14153–14172. PMLR, 2022.
- [24] Tongliang Liu and Dacheng Tao. Classification with noisy labels by importance reweighting. *IEEE Transactions on pattern analysis and machine intelligence*, 38(3):447–461, 2015.
- [25] Yang Liu. Understanding instance-level label noise: Disparate impacts and treatments. In *International Conference on Machine Learning*, pages 6725–6735. PMLR, 2021.
- [26] Yang Liu and Hongyi Guo. Peer loss functions: Learning from noisy labels without knowing noise rates. In *International Conference on Machine Learning*, pages 6226–6236. PMLR, 2020.
- [27] Michal Lukasik, Srinadh Bhojanapalli, Aditya Menon, and Sanjiv Kumar. Does label smoothing mitigate label noise? In *International Conference on Machine Learning*, pages 6448–6458. PMLR, 2020.
- [28] Scott M Lundberg and Su-In Lee. A unified approach to interpreting model predictions. In *Proceedings of the 31st international conference on neural information processing systems*, pages 4768–4777, 2017.
- [29] Tianyi Luo, Xingyu Li, Hainan Wang, and Yang Liu. Research replication prediction using weakly supervised learning. In *In Proceedings of the 2020 Conference on Empirical Methods in Natural Language Processing: Findings*, 2020.
- [30] Natalia Martinez, Martin Bertran, and Guillermo Sapiro. Fairness with minimal harm: A pareto-optimal approach for healthcare. *arXiv preprint arXiv:1911.06935*, 2019.
- [31] Aditya Menon, Brendan Van Rooyen, Cheng Soon Ong, and Bob Williamson. Learning from corrupted binary labels via class-probability estimation. In *International Conference on Machine Learning*, pages 125–134, 2015.
- [32] Aditya Krishna Menon, Sadeep Jayasumana, Ankit Singh Rawat, Himanshu Jain, Andreas Veit, and Sanjiv Kumar. Long-tail learning via logit adjustment. *arXiv preprint arXiv:2007.07314*, 2020.
- [33] Aditya Krishna Menon, Sadeep Jayasumana, Ankit Singh Rawat, Himanshu Jain, Andreas Veit, and Sanjiv Kumar. Long-tail learning via logit adjustment. In *International Conference on Learning Representations*, 2021.
- [34] Aditya Krishna Menon and Robert C Williamson. The cost of fairness in binary classification. In *Conference on Fairness, accountability and transparency*, pages 107–118. PMLR, 2018.
- [35] Nagarajan Natarajan, Inderjit S Dhillon, Pradeep K Ravikumar, and Ambuj Tewari. Learning with noisy labels. In *Advances in neural information processing systems*, pages 1196–1204, 2013.
- [36] Art B Owen. Sobol’ indices and shapley value. *SIAM/ASA Journal on Uncertainty Quantification*, 2(1):245–251, 2014.
- [37] Art B Owen and Clémentine Prieur. On shapley value for measuring importance of dependent inputs. *SIAM/ASA Journal on Uncertainty Quantification*, 5(1):986–1002, 2017.
- [38] Seulki Park, Jongin Lim, Younghan Jeon, and Jin Young Choi. Influence-balanced loss for imbalanced visual classification. In *Proceedings of the IEEE/CVF International Conference on Computer Vision*, pages 735–744, 2021.
- [39] Giorgio Patrini, Alessandro Rozza, Aditya Krishna Menon, Richard Nock, and Lizhen Qu. Making deep neural networks robust to label noise: A loss correction approach. In *Proceedings of the IEEE Conference on Computer Vision and Pattern Recognition*, pages 1944–1952, 2017.
- [40] Can Qin, Yizhou Wang, and Yun Fu. Robust semi-supervised domain adaptation against noisy labels. In *Proceedings of the 31st ACM International Conference on Information & Knowledge Management*, pages 4409–4413, 2022.
- [41] Jiawei Ren, Cunjun Yu, Shunan Sheng, Xiao Ma, Haiyu Zhao, Shuai Yi, and Hongsheng Li. Balanced meta-softmax for long-tailed visual recognition. *arXiv preprint arXiv:2007.10740*, 2020.
- [42] Marco Tulio Ribeiro, Sameer Singh, and Carlos Guestrin. " why should i trust you?" explaining the predictions of any classifier. In *Proceedings of the 22nd ACM SIGKDD international conference on knowledge discovery and data mining*, pages 1135–1144, 2016.

- [43] Ruslan Salakhutdinov, Antonio Torralba, and Josh Tenenbaum. Learning to share visual appearance for multiclass object detection. In *CVPR 2011*, pages 1481–1488. IEEE, 2011.
- [44] Clayton Scott. A rate of convergence for mixture proportion estimation, with application to learning from noisy labels. In *AISTATS*, 2015.
- [45] Clayton Scott, Gilles Blanchard, Gregory Handy, Sara Pozzi, and Marek Flaska. Classification with asymmetric label noise: Consistency and maximal denoising. In *COLT*, pages 489–511, 2013.
- [46] Hwanjun Song, Minseok Kim, and Jae-Gil Lee. Selfie: Refurbishing unclean samples for robust deep learning. In *International Conference on Machine Learning*, pages 5907–5915, 2019.
- [47] Mukund Sundararajan, Ankur Taly, and Qiqi Yan. Axiomatic attribution for deep networks. In *International Conference on Machine Learning*, pages 3319–3328. PMLR, 2017.
- [48] Berk Ustun, Yang Liu, and David Parkes. Fairness without harm: Decoupled classifiers with preference guarantees. In *International Conference on Machine Learning*, pages 6373–6382. PMLR, 2019.
- [49] Brendan Van Rooyen, Aditya Menon, and Robert C Williamson. Learning with symmetric label noise: The importance of being unhinged. In *Advances in Neural Information Processing Systems*, pages 10–18, 2015.
- [50] Jialu Wang, Yang Liu, and Caleb Levy. Fair classification with group-dependent label noise. *FACCT*, page 526–536, New York, NY, USA, 2021.
- [51] Jialu Wang, Xin Eric Wang, and Yang Liu. Understanding instance-level impact of fairness constraints. In *International Conference on Machine Learning*, pages 23114–23130. PMLR, 2022.
- [52] Hongxin Wei, Lei Feng, Xiangyu Chen, and Bo An. Combating noisy labels by agreement: A joint training method with co-regularization. In *Proceedings of the IEEE/CVF Conference on Computer Vision and Pattern Recognition*, pages 13726–13735, 2020.
- [53] Hongxin Wei, Lue Tao, Renchunzi Xie, and Bo An. Open-set label noise can improve robustness against inherent label noise. *Advances in Neural Information Processing Systems*, 34, 2021.
- [54] Hongxin Wei, Renchunzi Xie, Hao Cheng, Lei Feng, Bo An, and Yixuan Li. Mitigating neural network overconfidence with logit normalization. In *International Conference on Machine Learning*, pages 23631–23644. PMLR, 2022.
- [55] Hongxin Wei, Huiping Zhuang, Renchunzi Xie, Lei Feng, Gang Niu, Bo An, and Yixuan Li. Logit clipping for robust learning against label noise. *arXiv preprint arXiv:2212.04055*, 2022.
- [56] Jiaheng Wei, Hangyu Liu, Tongliang Liu, Gang Niu, and Yang Liu. Understanding generalized label smoothing when learning with noisy labels. *arXiv preprint arXiv:2106.04149*, 2021.
- [57] Jiaheng Wei and Yang Liu. When optimizing f -divergence is robust with label noise. In *International Conference on Learning Representations*, 2020.
- [58] Jiaheng Wei, Zhaowei Zhu, Hao Cheng, Tongliang Liu, Gang Niu, and Yang Liu. Learning with noisy labels revisited: A study using real-world human annotations. *arXiv preprint arXiv:2110.12088*, 2021.
- [59] Jiaheng Wei, Zhaowei Zhu, Hao Cheng, Tongliang Liu, Gang Niu, and Yang Liu. Learning with noisy labels revisited: A study using real-world human annotations. In *International Conference on Learning Representations*, 2022.
- [60] Tong Wei, Jiang-Xin Shi, Wei-Wei Tu, and Yu-Feng Li. Robust long-tailed learning under label noise. *arXiv preprint arXiv:2108.11569*, 2021.
- [61] Xiaobo Xia, Bo Han, Nannan Wang, Jiankang Deng, Jiatong Li, Yinian Mao, and Tongliang Liu. Extended- t : Learning with mixed closed-set and open-set noisy labels. *IEEE Transactions on Pattern Analysis and Machine Intelligence*, 2022.
- [62] Xiaobo Xia, Tongliang Liu, Bo Han, Chen Gong, Nannan Wang, Zongyuan Ge, and Yi Chang. Robust early-learning: Hindering the memorization of noisy labels. In *International conference on learning representations*, 2021.
- [63] Xiaobo Xia, Tongliang Liu, Bo Han, Mingming Gong, Jun Yu, Gang Niu, and Masashi Sugiyama. Instance correction for learning with open-set noisy labels. *arXiv preprint arXiv:2106.00455*, 2021.
- [64] Xiaobo Xia, Tongliang Liu, Bo Han, Mingming Gong, Jun Yu, Gang Niu, and Masashi Sugiyama. Sample selection with uncertainty of losses for learning with noisy labels. *arXiv preprint arXiv:2106.00445*, 2021.
- [65] Tong Xiao, Tian Xia, Yi Yang, Chang Huang, and Xiaogang Wang. Learning from massive noisy labeled data for image classification. In *Proceedings of the IEEE Conference on Computer Vision and Pattern Recognition*, pages 2691–2699, 2015.

- [66] Jingfeng Zhang, Xilie Xu, Bo Han, Tongliang Liu, Lizhen Cui, Gang Niu, and Masashi Sugiyama. Noilin: Improving adversarial training and correcting stereotype of noisy labels. 2022.
- [67] Yifan Zhang, Bingyi Kang, Bryan Hooi, Shuicheng Yan, and Jiashi Feng. Deep long-tailed learning: A survey. *arXiv preprint arXiv:2110.04596*, 2021.
- [68] Han Zhao and Geoff Gordon. Inherent tradeoffs in learning fair representations. *Advances in neural information processing systems*, 32, 2019.
- [69] Yaoyao Zhong, Weihong Deng, Mei Wang, Jiani Hu, Jianteng Peng, Xunqiang Tao, and Yaohai Huang. Unequal-training for deep face recognition with long-tailed noisy data. In *Proceedings of the IEEE/CVF Conference on Computer Vision and Pattern Recognition*, pages 7812–7821, 2019.
- [70] Xiangxin Zhu, Dragomir Anguelov, and Deva Ramanan. Capturing long-tail distributions of object subcategories. In *Proceedings of the IEEE Conference on Computer Vision and Pattern Recognition*, pages 915–922, 2014.
- [71] Zhaowei Zhu, Zihao Dong, and Yang Liu. Detecting corrupted labels without training a model to predict. In *International Conference on Machine Learning*, pages 27412–27427. PMLR, 2022.
- [72] Zhaowei Zhu, Tongliang Liu, and Yang Liu. A second-order approach to learning with instance-dependent label noise. In *The IEEE Conference on Computer Vision and Pattern Recognition (CVPR)*, June 2021.
- [73] Zhaowei Zhu, Tianyi Luo, and Yang Liu. The rich get richer: Disparate impact of semi-supervised learning. *arXiv preprint arXiv:2110.06282*, 2021.
- [74] Zhaowei Zhu, Yiwen Song, and Yang Liu. Clusterability as an alternative to anchor points when learning with noisy labels. *arXiv preprint arXiv:2102.05291*, 2021.
- [75] Zhaowei Zhu, Jialu Wang, and Yang Liu. Beyond images: Label noise transition matrix estimation for tasks with lower-quality features. *arXiv preprint arXiv:2202.01273*, 2022.

Appendix

The Appendix is organized as follows.

- Section A theoretically demonstrates why special treatments on sub-populations are necessary, and why **Fairness Regularizer (FR)** improves learning from the noisily labeled long-tailed data.
- Section B includes all omitted proofs for theoretical conclusions.
- Section C gives additional experiment details and results.

A Long-Tailed Sub-Populations Deserve Special Treatments

In light of the empirical observations, we now theoretically explore the impacts of sub-populations when learning with long-tailed noisy data, through a binary Gaussian example. Note that classes could be viewed as a special case of sub-populations, we adopt the class-level long-tailed distributions for illustration.

A.1 Formulation

Consider the binary classification task such that $K = 2$, and the data samples are generated by P_{XY} , which is the mixture of two Gaussians. Suppose $X^\pm := (X|Y = \pm 1) \sim \mathcal{N}(\mu_\pm, \sigma^2)$ where \mathcal{N} is the Gaussian distribution, and $\mathbb{P}(Y = +1) = \mathbb{P}(Y = -1)$. W.l.o.g., we assume that $\mu_+ > \mu_-$. Suppose a classifier f was trained on the noisy (and potentially imbalanced/long-tailed) training data $X_I := \{x_i\}_{i=1}^n$ where the corresponding noisy label of x_i is $\tilde{y}_i \in \tilde{Y}$, $\forall i \in [n]$. Samples x_i were drawn non-uniformly (i.e., imbalance) from X , and the ground-truth label of samples x_i is y_i given by Y .

To inspect on the influence of sub-populations, we further split the imbalanced noisily labeled training data into two parts by referring to their clean labels: head-Gaussian data and tail-Gaussian data. For $x_i \sim X^\pm, y \in \{\pm 1\}$, we denote the set of head and tail data in class ± 1 as $S_H^\pm := X_I \cap X_H^\pm, S_T^\pm := X_I \cap X_T^\pm$, where $X_H^\pm := \{x \sim X^\pm | \frac{x - \mu_\pm}{\sigma} \cdot y \geq -\eta\}$, $X_T^\pm := \{x \sim X^\pm | \frac{x - \mu_\pm}{\sigma} \cdot y < -\eta\}$ respectively. To clarify, replacing all “ \pm ” symbols by $+1$ will return the notation for class $+1$. And $G \in \{H, T\}$ in this setting.

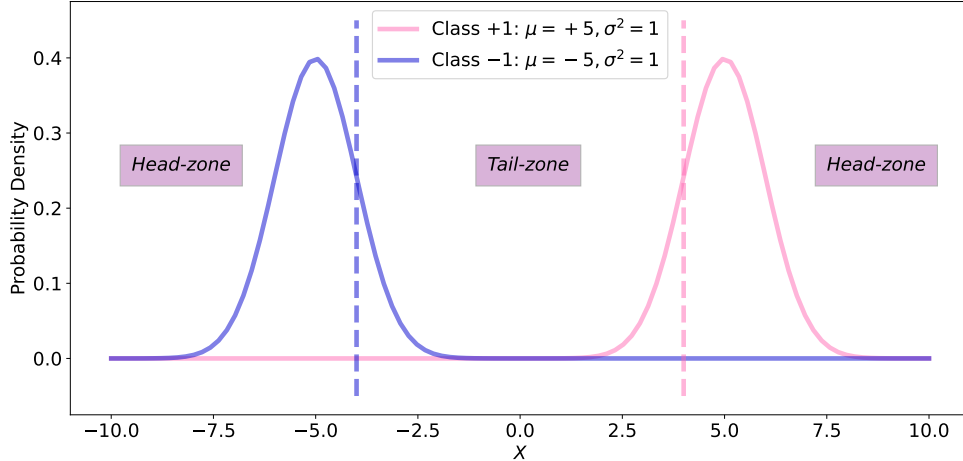


Figure 7: An illustration of head/tail separations: when $\mu_+ = +5, \mu_- = -5, \sigma^2 = 1, \eta = 1$, the probability density distribution of Class +1 (Pink) and Class -1 (Blue) are drawn. x -axis indicates the Gaussian samples drawn from two Gaussian distributions, y -axis is the corresponding probability density of samples being equal to x .

In the view of sub-populations, we assume that the noise transition differs w.r.t. the head and tail proportion, since tail populations are more misleading in the classification (i.e., in Figure 7, the label of samples in the “tail-zone” is more likely to be wrongly given). Assume that the noise transition matrix in the head samples and tail samples follow T_H, T_T respectively:

$$T_H = \begin{pmatrix} 1 - \rho_H^- & \rho_H^- \\ \rho_H^+ & 1 - \rho_H^+ \end{pmatrix}, \quad T_T = \begin{pmatrix} 1 - \rho_T^- & \rho_T^- \\ \rho_T^+ & 1 - \rho_T^+ \end{pmatrix}.$$

To refer to the noisy labels, we add the $\tilde{\cdot}$ sign for the notations that are w.r.t. \tilde{Y} instead of Y : i.e., $\tilde{X}^\pm := (X|\tilde{Y} = \pm 1)$, $\tilde{S}_H^\pm := X_I \cap \tilde{X}_H^\pm$ with $\tilde{X}_H^\pm := \{x \sim \tilde{X}^\pm | \frac{x - \mu_\pm}{\sigma} \cdot \tilde{y} \geq -\eta\}$, etc. W.l.o.g., we assume that the noise rates are not too large, i.e., $\rho_H^\pm, \rho_T^\pm \in [0.0, 0.5)$. Besides, we are interested in the scenario where the ground-truth samples are imbalanced. And we can assume that the imbalance ratio $r := \frac{|S_H^+| + |S_T^+|}{|S_H^-| + |S_T^-|}$ satisfies $r > 1$.

A.2 The Error Probability

Given a classifier f , the *Error probability* is defined as the percentage of error rates under a given data distribution:

Definition A.1 (Error probability). The error probability of a classifier f on the data distribution (X, Y) is defined as $\text{Err}_X(f) := \mathbb{P}_{(X, Y)}(f(X) \neq Y)$.

Denote by Φ the cumulative distribution function (CDF) of the standard Gaussian distribution $\mathcal{N}(0, 1)$, we derive the error probability for the four populations as:

Proposition A.2. For any linear classifier of the form $f(x) = \text{sign}(x - \theta)$, we have:

$$\text{Err}_{X_T^\pm}(f) - \text{Err}_{X_H^\pm}(f) \propto \Phi((\theta - \mu_\pm) \cdot (\pm 1)) \cdot \text{sign}((\mu_\pm - \theta) \cdot (\pm 1) - \eta\sigma).$$

μ_\pm denotes the mean of two Gaussians and the Bayes optimal classifier adopts the threshold $\theta^* := \frac{\mu_- + \mu_+}{2}$. We take the tail class -1 (replace all symbols “ \pm ” by “ $-$ ”) as an illustration:

- When $\theta \geq \mu_- + \eta\sigma$, the error probability gap $\text{Err}_{X_T^-}(f) - \text{Err}_{X_H^-}(f)$ is monotonically increasing w.r.t. the increase of $\Phi((\theta - \mu_-)) \cdot \text{sign}((\theta - \mu_-) - \eta\sigma) = \Phi((\theta - \mu_-))$. Without additional treatments, the classifier over-fits on the head class to achieve a lower error probability. As a result, θ decreases, and the error gap between two populations in the tail class enlarges.
- When θ decreases small enough, i.e., $\theta < \mu_- + \eta\sigma$, the error probability gap $\text{Err}_{X_T^-}(f) - \text{Err}_{X_H^-}(f)$ is monotonically increasing w.r.t. the increase of $-\Phi((\theta - \mu_-))$. Further decreasing θ will make both populations in the tail class yield a large error probability.

A.3 The Bias of The Estimator

We next adopt the estimation bias as a metric to show how class-imbalance and noisy labels degrade the model performance of estimated classifier f . The following proposition captures the influence of each sub-population on the bias of the estimator, compared to the Bayes optimal classifier.

Proposition A.3. Denote the estimator on the imbalanced noisy data \tilde{X}_I as $\tilde{f}^* = \text{sign}(x - \tilde{\theta})$, $\forall \delta > 0$, with probability at least p , $\text{Bias} := \frac{\mu_- - \mu_+}{2} \cdot \left(\frac{\rho_H^+ |\tilde{S}_H^+| + \rho_T^+ |\tilde{S}_T^+|}{|\tilde{S}_H^+| + |\tilde{S}_T^+|} - \frac{\rho_H^- |\tilde{S}_H^-| + \rho_T^- |\tilde{S}_T^-|}{|\tilde{S}_H^-| + |\tilde{S}_T^-|} \right)$, we have:

$$\text{Bias} - \delta \leq \left| \tilde{\theta} - \theta^* \right| \leq \text{Bias} + \delta.$$

We defer the form of p till the proof of Proposition A.3 to not complicate the presentation. Briefly speaking, p is large when (i) sample complexity is rich (large $|\tilde{S}_I^\pm|$); (ii) balanced class ($|\tilde{S}_I^+| \rightarrow |\tilde{S}_I^-|$); or (iii) balanced sub-populations ($|\tilde{S}_H^\pm| \rightarrow |\tilde{S}_T^\pm|$). Going contrary to any above-mentioned scenario will result in a smaller probability p to obtain a high-qualified estimator.

Remark A.4. The term Bias indicates the quality/distance of the estimator by referring to the threshold θ^* of Bayes optimal classifier f^* . The term Bias reduces to 0 and $\tilde{\theta} = \hat{\theta} = \theta^*$ when T_T and T_H have all zero off-diagonal elements. And non-zero off-diagonal entries of noise transition matrices are likely to return a biased estimator ($\text{Bias} \neq 0$). $\tilde{\theta}$ shifts away from the class with a lower weighted noise rate of the noisy labels to achieve a low error probability. Moreover, note that with the presence of label noise, the non-zero difference of the population level noise rate as well as the sample complexity further exerts differed impacts of sub-populations on the estimator.

A.4 Why Does FR Help with Improvements

Building upon the previous discussions, to show why **FR** helps with improving the learning, we first derive the per sub-population error probability w.r.t. the noisy labels, since in practice, clean labels are not available for the **FR** to constrain.

Lemma A.5. *The error probability of a classifier f on the per-population noisy data distribution (X, \widetilde{Y}) could be expressed in the forms of error probabilities under the clean data distribution, specifically:*

$$\begin{aligned} \text{Err}_{X_H^+}^{\sim}(f) &= p \cdot (1 - \rho_H^+) \cdot \text{Err}_{X_H^+} + (1 - p) \cdot \rho_H^- \cdot (1 - \text{Err}_{X_H^-}); \\ \text{Err}_{X_H^-}^{\sim}(f) &= p \cdot \rho_H^+ \cdot \text{Err}_{X_H^+} + (1 - p) \cdot (1 - \rho_H^-) \cdot (1 - \text{Err}_{X_H^-}); \\ \text{Err}_{X_T^+}^{\sim}(f) &= p \cdot (1 - \rho_T^+) \cdot \text{Err}_{X_T^+} + (1 - p) \cdot \rho_T^- \cdot (1 - \text{Err}_{X_T^-}); \\ \text{Err}_{X_T^-}^{\sim}(f) &= p \cdot \rho_T^+ \cdot \text{Err}_{X_T^+} + (1 - p) \cdot (1 - \rho_T^-) \cdot (1 - \text{Err}_{X_T^-}). \end{aligned}$$

Although the overall error probability on the clean data distribution is:

$$\text{Err}(f) := \mathbb{P}(X_H^+) \cdot \text{Err}_{X_H^+}(f) + \mathbb{P}(X_H^-) \cdot \text{Err}_{X_H^-}(f) + \mathbb{P}(X_T^+) \cdot \text{Err}_{X_T^+}(f) + \mathbb{P}(X_T^-) \cdot \text{Err}_{X_T^-}(f).$$

when learning with noisy data distribution with imbalanced sub-populations, the optimal f w.r.t. the noisy data distribution is supposed to be given by the optimum of the following Risk Minimization:

$$\text{RM: } \min_f \widetilde{\text{Err}}(f) := \mathbb{P}(\widetilde{X}_H^+) \cdot \text{Err}_{X_H^+}^{\sim}(f) + \mathbb{P}(\widetilde{X}_H^-) \cdot \text{Err}_{X_H^-}^{\sim}(f) + \mathbb{P}(\widetilde{X}_T^+) \cdot \text{Err}_{X_T^+}^{\sim}(f) + \mathbb{P}(\widetilde{X}_T^-) \cdot \text{Err}_{X_T^-}^{\sim}(f).$$

To distinguish the overall error probability under noisy and clean data distribution, we offer Theorem A.6:

Theorem A.6. *When $\mathbb{P}(Y = +1) = \mathbb{P}(Y = -1)$, an equivalent form of the minimization w.r.t. $\widetilde{\text{Err}}(f)$ is characterized by:*

$$\min_f \widetilde{\text{Err}}(f) \iff \min_f \text{Err}(f) - 2r \cdot \rho_H \cdot \left(\text{Err}_{X_H^+}^{\sim}(f) - \text{Err}_{X_H^-}^{\sim}(f) \right) - \rho_T \cdot \left(\text{Err}_{X_T^+}^{\sim}(f) - \text{Err}_{X_T^-}^{\sim}(f) \right),$$

where we define the noise rate gaps as $\rho_H := \rho_H^+ - \rho_H^-$, $\rho_T := \rho_T^+ - \rho_T^-$, and the sub-population imbalance ratio as $r := \frac{1 - \Phi(-\eta)}{\Phi(-\eta)}$.

Thus, constraining the classifier to perform fair performances (i.e., same training error probabilities such as $\text{Err}_{X_H^+}^{\sim}(f) = \text{Err}_{X_H^-}^{\sim}(f)$, and $\text{Err}_{X_T^+}^{\sim}(f) = \text{Err}_{X_T^-}^{\sim}(f)$), the optimal classifier training on the noisy data distribution with fairness regularizer yields the optimal classifier by refer to the clean data distribution! We then have:

Corollary A.7. *When $\mathbb{P}(Y = +1) = \mathbb{P}(Y = -1)$, **FR** constrains the error probability (performance gap) between \widetilde{X}_H^+ and \widetilde{X}_H^- , \widetilde{X}_T^+ and \widetilde{X}_T^- . As a result, $\min_f \widetilde{\text{Err}}(f) \iff \min_f \text{Err}(f)$.*

The proof is straightforward from the result in Theorem A.6.

B Omitted Proofs

B.1 Proof of Proposition A.2

Proof. For the head population in Class +1, we can derive the error probability as:

$$\text{Err}_{X_H^+}(f) := \mathbb{P}_{(X_H^+, Y)}(f(X_H^+) \neq Y) = \mathbb{P}_{(X_H^+, Y)}((X_H^+ - \theta)Y < 0) = \mathbb{P}_{(X_H^+, Y)}(X_H^+ < \theta).$$

Due to the separation of head and tail in Class +1, we then have:

$$\begin{aligned} \text{Err}_{X_H^+}(f) &= \frac{\mathbb{P}_{x \sim \mathcal{N}(\mu_+, \sigma^2)}(x < \theta, \frac{x - \mu_+}{\sigma} \geq -\eta)}{\mathbb{P}_{x \sim \mathcal{N}(\mu_+, \sigma^2)}(\frac{x - \mu_+}{\sigma} \geq -\eta)} \\ &= \frac{\mathbb{P}(\mathcal{N}(\mu_+, \sigma^2) < \theta, \mathcal{N}(0, \sigma^2) \geq -\eta\sigma)}{\mathbb{P}(\mathcal{N}(0, 1) \geq -\eta)} \\ &= \frac{\mathbb{P}(\mathcal{N}(0, 1) < \frac{\theta - \mu_+}{\sigma}, \mathcal{N}(0, 1) \geq -\eta)}{1 - \Phi(-\eta)}. \end{aligned}$$

where we denote by Φ the CDF of the standard Gaussian distribution $\mathcal{N}(0, 1)$, and $\Phi(a) = 1 - \Phi(-a)$. Similarly, for the tail population in Class +1, we can derive the error probability as:

$$\begin{aligned}
\text{Err}_{X_T^+}(f) &:= \mathbb{P}_{(X_T^+, Y)}(f(X_T^+) \neq Y) = \mathbb{P}_{(X_T^+, Y)}((X_T^+ - \theta)Y < 0) = \mathbb{P}_{(X_T^+, Y)}(X_T^+ < \theta) \\
&= \frac{\mathbb{P}_{x \sim \mathcal{N}(\mu_+, \sigma^2)}(x < \theta, \frac{x - \mu_+}{\sigma} < -\eta)}{\mathbb{P}_{x \sim \mathcal{N}(\mu_+, \sigma^2)}(\frac{x - \mu_+}{\sigma} < -\eta)} \\
&= \frac{\mathbb{P}(\mathcal{N}(\mu_+, \sigma^2) < \theta, \mathcal{N}(0, \sigma^2) < -\eta\sigma)}{\mathbb{P}(\mathcal{N}(0, 1) < -\eta)} \\
&= \frac{\mathbb{P}(\mathcal{N}(0, 1) < \frac{\theta - \mu_+}{\sigma}, \mathcal{N}(0, 1) < -\eta)}{\Phi(-\eta)}.
\end{aligned}$$

For the populations in Class -1, we have:

$$\begin{aligned}
\text{Err}_{X_H^-}(f) &:= \mathbb{P}_{(X_H^-, Y)}(f(X_H^-) \neq Y) = \mathbb{P}_{(X_H^-, Y)}((X_H^- - \theta)Y > 0) = \mathbb{P}_{(X_H^-, Y)}(X_H^- > \theta) \\
&= \frac{\mathbb{P}_{x \sim \mathcal{N}(\mu_-, \sigma^2)}(x > \theta, \frac{x - \mu_-}{\sigma} \leq \eta)}{\mathbb{P}_{x \sim \mathcal{N}(\mu_-, \sigma^2)}(\frac{x - \mu_-}{\sigma} \leq \eta)} \\
&= \frac{\mathbb{P}(\mathcal{N}(\mu_-, \sigma^2) > \theta, \mathcal{N}(0, \sigma^2) \leq \eta\sigma)}{\mathbb{P}(\mathcal{N}(0, 1) \leq \eta)} \\
&= \frac{\mathbb{P}(\mathcal{N}(0, 1) > \frac{\theta - \mu_-}{\sigma}, \mathcal{N}(0, 1) \leq \eta)}{1 - \Phi(-\eta)}.
\end{aligned}$$

$$\begin{aligned}
\text{Err}_{X_T^-}(f) &:= \mathbb{P}_{(X_T^-, Y)}(f(X_T^-) \neq Y) \\
&= \mathbb{P}_{(X_T^-, Y)}((X_T^- - \theta)Y > 0) \\
&= \mathbb{P}_{(X_T^-, Y)}(X_T^- > \theta) \\
&= \frac{\mathbb{P}_{x \sim \mathcal{N}(\mu_-, \sigma^2)}(x > \theta, \frac{x - \mu_-}{\sigma} > \eta)}{\mathbb{P}_{x \sim \mathcal{N}(\mu_-, \sigma^2)}(\frac{x - \mu_-}{\sigma} > \eta)} \\
&= \frac{\mathbb{P}(\mathcal{N}(\mu_-, \sigma^2) > \theta, \mathcal{N}(0, \sigma^2) > \eta\sigma)}{\mathbb{P}(\mathcal{N}(0, 1) > \eta)} \\
&= \frac{\mathbb{P}(\mathcal{N}(0, 1) > \frac{\theta - \mu_-}{\sigma}, \mathcal{N}(0, 1) > \eta)}{\Phi(-\eta)}.
\end{aligned}$$

The above thresholds can be further simplified into following forms given the cumulative distribution function (CDF) of the normal Gaussian distribution. If $\theta \leq \mu_+ - \eta\sigma$, then:

$$\text{Err}_{X_H^+}(f) = \frac{0}{1 - \Phi(-\eta)} = 0, \quad \text{Err}_{X_T^+}(f) = \frac{\mathbb{P}(\mathcal{N}(0, 1) < \min(\frac{\theta - \mu_+}{\sigma}, -\eta))}{\Phi(-\eta)} = \frac{\Phi(\frac{\theta - \mu_+}{\sigma})}{\Phi(-\eta)};$$

otherwise, we have $\theta > \mu_+ - \eta\sigma$ and:

$$\text{Err}_{X_H^+}(f) = \frac{\mathbb{P}(-\eta \leq \mathcal{N}(0, 1) < \frac{\theta - \mu_+}{\sigma})}{1 - \Phi(-\eta)} = \frac{\Phi(\frac{\theta - \mu_+}{\sigma}) - \Phi(-\eta)}{1 - \Phi(-\eta)}, \quad \text{Err}_{X_T^+}(f) = 1.$$

As for the class -1, when $\theta \geq \mu_- + \eta\sigma$, we obtain:

$$\text{Err}_{X_H^-}(f) = \frac{0}{1 - \Phi(-\eta)} = 0, \quad \text{Err}_{X_T^-}(f) = \frac{\mathbb{P}(\mathcal{N}(0, 1) > \max(\frac{\theta - \mu_-}{\sigma}, \eta))}{\Phi(-\eta)} = \frac{\Phi(\frac{\mu_- - \theta}{\sigma})}{\Phi(-\eta)};$$

otherwise, we have $\theta < \mu_- + \eta\sigma$ and:

$$\text{Err}_{X_H^-}(f) = \frac{\mathbb{P}(\frac{\theta - \mu_-}{\sigma} < \mathcal{N}(0, 1) \leq \eta)}{1 - \Phi(-\eta)} = \frac{\Phi(\frac{\mu_- - \theta}{\sigma}) - \Phi(-\eta)}{1 - \Phi(-\eta)}, \quad \text{Err}_{X_T^-}(f) = 1.$$

We take Class -1 for illustration, when $\theta \geq \mu_- + \eta\sigma$, we have: $(\mu_- - \theta) \cdot (-1) - \eta\sigma \geq 0$. In this case, the difference of error probabilities in tail and head populations becomes:

$$\begin{aligned} \text{Err}_{X_T^-}(f) - \text{Err}_{X_H^-}(f) &= \frac{\Phi\left(\frac{\mu_- - \theta}{\sigma}\right)}{\Phi(-\eta)} \propto \Phi\left(\frac{\mu_- - \theta}{\sigma}\right) \propto \Phi(\mu_- - \theta) \\ &\propto \Phi((\theta - \mu_-) \cdot (-1)) \cdot \text{sign}((\mu_- - \theta) \cdot (-1) - \eta\sigma). \end{aligned}$$

When $\theta < \mu_- + \eta\sigma$, we have: $(\mu_- - \theta) \cdot (-1) - \eta\sigma < 0$. In this case, the difference of error probabilities in tail and head populations becomes:

$$\begin{aligned} \text{Err}_{X_T^-}(f) - \text{Err}_{X_H^-}(f) &= 1 - \frac{\Phi\left(\frac{\mu_- - \theta}{\sigma}\right) - \Phi(-\eta)}{1 - \Phi(-\eta)} \\ &= \frac{1 - \Phi\left(\frac{\mu_- - \theta}{\sigma}\right)}{1 - \Phi(-\eta)} \\ &= \frac{\Phi\left(\frac{\theta - \mu_-}{\sigma}\right)}{1 - \Phi(-\eta)} \propto \Phi\left(\frac{\theta - \mu_-}{\sigma}\right) \propto \Phi(\mu_- - \theta) \cdot (-1) \\ &\propto \Phi((\theta - \mu_-) \cdot (-1)) \cdot \text{sign}((\mu_- - \theta) \cdot (-1) - \eta\sigma). \end{aligned}$$

For Class $+1$, the conclusion could be derived similarly. \square

B.2 Proof of Proposition A.3

Proof. For sample $X_i \in \tilde{S}_1^+ := \tilde{S}_H^+ \cup \tilde{S}_T^+$, we express X_i by $X_i = (1 - I_i^+)(\mu_- - \mu_+) + Z_i^+$, where $Z_i^+ \sim \mathcal{N}(\mu_+, \sigma^2)$ and I_i^+ satisfies that:

$$\begin{aligned} \text{If } X_i \in \tilde{S}_T^+ : \quad & \frac{z_i^+ - \mu_+}{\sigma} < -\eta, \quad I_i^+ \sim \text{Bernoulli}[\tilde{A}_T^+]; \\ \text{If } X_i \in \tilde{S}_H^+ : \quad & \frac{z_i^+ - \mu_+}{\sigma} \geq -\eta, \quad I_i^+ \sim \text{Bernoulli}[\tilde{A}_H^+], \end{aligned}$$

and $\tilde{A}_H^+ := 1 - \rho_H^+$, $\tilde{A}_T^+ := 1 - \rho_T^+$ indicate the accuracy of noisy labels/annotations for the two populations in class $+1$.

Similarly, for sample $X_i \in \tilde{S}_1^- := \tilde{S}_H^- \cup \tilde{S}_T^-$, we express X_i by $X_i = (1 - I_i^-)(\mu_+ - \mu_-) + Z_i^-$, where $Z_i^- \sim \mathcal{N}(\mu_-, \sigma^2)$ and I_i^- satisfies that:

$$\begin{aligned} \text{If } X_i \in \tilde{S}_T^- : \quad & \frac{z_i^- - \mu_-}{\sigma} > \eta, \quad I_i^- \sim \text{Bernoulli}[\tilde{A}_T^-]; \\ \text{If } X_i \in \tilde{S}_H^- : \quad & \frac{z_i^- - \mu_-}{\sigma} \leq \eta, \quad I_i^- \sim \text{Bernoulli}[\tilde{A}_H^-], \end{aligned}$$

with $\tilde{A}_H^- := 1 - \rho_H^+$, $\tilde{A}_T^- := 1 - \rho_T^+$ being the accuracy of noisy labels/annotations for the two populations in class -1 .

To illustrate the quantities, we take $X_i \in \tilde{S}_1^+$ as an example. I_i^+ can be viewed as the random variable of the correct annotations in a Bernoulli trial, where there only two outcomes: correct annotation and wrong annotation. If the noisy label \tilde{Y}_i of X_i is correct, i.e., $\tilde{Y}_i = Y_i$, we have $I_i^+ = 1$ and: $X_i = (1 - 1)(\mu_- - \mu_+) + Z_i^+ = Z_i^+$. Otherwise, we have $\tilde{Y}_i \neq Y_i$, and $X_i = (1 - 0)(\mu_- - \mu_+) + Z_i^+ = Z_i^-$.

Now we switch our focus on the accuracy of estimator $\tilde{\theta}$:

$$\begin{aligned} 2\tilde{\theta} &= \sum_{X_i \in \tilde{S}_1^+} \frac{X_i}{|\tilde{S}_1^+|} + \sum_{X_i \in \tilde{S}_1^-} \frac{X_i}{|\tilde{S}_1^-|} \\ &= \sum_{X_i \in \tilde{S}_1^+} \frac{(1 - I_i^+)(\mu_- - \mu_+) + Z_i^+}{|\tilde{S}_1^+|} + \sum_{X_i \in \tilde{S}_1^-} \frac{(1 - I_i^-)(\mu_+ - \mu_-) + Z_i^-}{|\tilde{S}_1^-|} \\ &= \left(\sum_{X_i \in \tilde{S}_1^+} \frac{I_i^+(\mu_+ - \mu_-)}{|\tilde{S}_1^+|} + \sum_{X_i \in \tilde{S}_1^-} \frac{I_i^-(\mu_- - \mu_+)}{|\tilde{S}_1^-|} \right) + \underbrace{\left(\sum_{X_i \in \tilde{S}_1^+} \frac{Z_i^+}{|\tilde{S}_1^+|} + \sum_{X_i \in \tilde{S}_1^-} \frac{Z_i^-}{|\tilde{S}_1^-|} \right)}_{\sim \mathcal{N}(\mu_+ + \mu_-, ((|\tilde{S}_1^+| + |\tilde{S}_1^-|)\sigma^2) / (|\tilde{S}_1^+| |\tilde{S}_1^-|))}. \end{aligned}$$

Define

$$\text{Bias} = \frac{\mu_- - \mu_+}{2} \left(-\frac{\widetilde{A}_H^+ |\widetilde{S}_H^+| + \widetilde{A}_T^+ |\widetilde{S}_T^+|}{|\widetilde{S}_T^+|} + \frac{\widetilde{A}_H^- |\widetilde{S}_H^-| + \widetilde{A}_T^- |\widetilde{S}_T^-|}{|\widetilde{S}_T^-|} \right),$$

we have:

$$\begin{aligned} & |2\widehat{\theta} - (\mu_+ + \mu_-) - 2\text{Bias}| \\ &= \left| \left(\sum_{X_i \in \widetilde{S}_H^+} \frac{I_i^+(\mu_+ - \mu_-)}{|\widetilde{S}_T^+|} + \sum_{X_i \in \widetilde{S}_T^+} \frac{I_i^+(\mu_+ - \mu_-)}{|\widetilde{S}_T^+|} + \sum_{X_i \in \widetilde{S}_H^-} \frac{I_i^-(\mu_- - \mu_+)}{|\widetilde{S}_T^-|} + \sum_{X_i \in \widetilde{S}_T^-} \frac{I_i^-(\mu_- - \mu_+)}{|\widetilde{S}_T^-|} - \text{Bias} \right) \right. \\ &\quad \left. + \left(\sum_{X_i \in \widetilde{S}_T^+} \frac{Z_i^+}{|\widetilde{S}_T^+|} + \sum_{X_i \in \widetilde{S}_T^-} \frac{Z_i^-}{|\widetilde{S}_T^-|} - (\mu_+ + \mu_-) \right) \right| \\ &= \left| (\mu_+ - \mu_-) \left(\sum_{X_i \in \widetilde{S}_H^+} \frac{I_i^+}{|\widetilde{S}_T^+|} - \frac{\widetilde{A}_H^+ |\widetilde{S}_H^+|}{|\widetilde{S}_T^+|} \right) + (\mu_+ - \mu_-) \left(\sum_{X_i \in \widetilde{S}_T^+} \frac{I_i^+}{|\widetilde{S}_T^+|} - \frac{\widetilde{A}_T^+ |\widetilde{S}_T^+|}{|\widetilde{S}_T^+|} \right) \right. \\ &\quad \left. + (\mu_- - \mu_+) \left(\sum_{X_i \in \widetilde{S}_H^-} \frac{I_i^-}{|\widetilde{S}_T^-|} - \frac{\widetilde{A}_H^- |\widetilde{S}_H^-|}{|\widetilde{S}_T^-|} \right) + (\mu_- - \mu_+) \left(\sum_{X_i \in \widetilde{S}_T^-} \frac{I_i^-}{|\widetilde{S}_T^-|} - \frac{\widetilde{A}_T^- |\widetilde{S}_T^-|}{|\widetilde{S}_T^-|} \right) \right. \\ &\quad \left. + \left(\sum_{X_i \in \widetilde{S}_T^+} \frac{Z_i^+}{|\widetilde{S}_T^+|} + \sum_{X_i \in \widetilde{S}_T^-} \frac{Z_i^-}{|\widetilde{S}_T^-|} - (\mu_+ + \mu_-) \right) \right| \\ &\leq \underbrace{|\mu_+ - \mu_-| \left| \frac{\sum_{X_i \in \widetilde{S}_H^+} I_i^+}{|\widetilde{S}_T^+|} - \frac{\widetilde{A}_H^+ |\widetilde{S}_H^+|}{|\widetilde{S}_T^+|} \right|}_{\text{Term ①}} + \underbrace{|\mu_+ - \mu_-| \left| \frac{\sum_{X_i \in \widetilde{S}_T^+} I_i^+}{|\widetilde{S}_T^+|} - \frac{\widetilde{A}_T^+ |\widetilde{S}_T^+|}{|\widetilde{S}_T^+|} \right|}_{\text{Term ②}} \\ &\quad + \underbrace{|\mu_- - \mu_+| \left| \frac{\sum_{X_i \in \widetilde{S}_H^-} I_i^-}{|\widetilde{S}_T^-|} - \frac{\widetilde{A}_H^- |\widetilde{S}_H^-|}{|\widetilde{S}_T^-|} \right|}_{\text{Term ③}} + \underbrace{|\mu_- - \mu_+| \left| \frac{\sum_{X_i \in \widetilde{S}_T^-} I_i^-}{|\widetilde{S}_T^-|} - \frac{\widetilde{A}_T^- |\widetilde{S}_T^-|}{|\widetilde{S}_T^-|} \right|}_{\text{Term ④}} \\ &\quad + \underbrace{\left| \left(\sum_{X_i \in \widetilde{S}_T^+} \frac{Z_i^+}{|\widetilde{S}_T^+|} + \sum_{X_i \in \widetilde{S}_T^-} \frac{Z_i^-}{|\widetilde{S}_T^-|} \right) - (\mu_+ + \mu_-) \right|}_{\text{Term ⑤}}. \end{aligned}$$

By using the Hoeffding inequality, for some $\epsilon > 0$, we have the following inequality for the head data:

$$\mathbb{P} \left(\left| \sum_{X_i \in \widetilde{S}_H^+} I_i^+ - \widetilde{A}_H^+ \cdot |\widetilde{S}_H^+| \right| > \epsilon |\widetilde{S}_H^+| \right) \leq 2e^{-2\epsilon^2 |\widetilde{S}_H^+|},$$

which is equivalent to:

$$\mathbb{P} \left(\left| \frac{\sum_{X_i \in \widetilde{S}_H^+} I_i^+}{|\widetilde{S}_T^+|} - \frac{\widetilde{A}_H^+ |\widetilde{S}_H^+|}{|\widetilde{S}_T^+|} \right| > \frac{|\widetilde{S}_H^+|}{|\widetilde{S}_T^+|} \epsilon \right) \leq 2e^{-2\epsilon^2 |\widetilde{S}_H^+|}.$$

Mapping $\epsilon \leftarrow \frac{|\widetilde{S}_H^+|}{|\widetilde{S}_T^+|} \epsilon$, the above inequality further becomes:

$$\mathbb{P} \left(\left| \frac{\sum_{X_i \in \widetilde{S}_H^+} I_i^+}{|\widetilde{S}_T^+|} - \frac{\widetilde{A}_H^+ |\widetilde{S}_H^+|}{|\widetilde{S}_T^+|} \right| > \epsilon \right) \leq 2e^{-2\epsilon^2 |\widetilde{S}_T^+|^2 / |\widetilde{S}_H^+|}.$$

Thus, for Term ① and $\epsilon = \frac{2\delta}{5|\mu_+ - \mu_-|}$, we have the following bound:

$$\mathbb{P} \left(\frac{1}{2} |\mu_+ - \mu_-| \underbrace{\left| \frac{\sum_{X_i \in \widetilde{S}_H^+} I_i^+}{|\widetilde{S}_T^+|} - \frac{\widetilde{A}_H^+ |\widetilde{S}_H^+|}{|\widetilde{S}_T^+|} \right|}_{\text{Term ①}} > \frac{\delta}{5} \right) \leq 2e^{-\frac{8\delta^2 |\widetilde{S}_T^+|^2}{25(\mu_+ - \mu_-)^2 |\widetilde{S}_H^+|}}.$$

For the tail data in \tilde{S}_1^+ , we can similarly obtain:

$$\mathbb{P}\left(\left|\frac{\sum_{X_i \in \tilde{S}_T^+} I_i^+}{|\tilde{S}_1^+|} - \tilde{A}_T^+ \frac{|\tilde{S}_T^+|}{|\tilde{S}_1^+|}\right| > \epsilon\right) \leq 2e^{-2\epsilon^2 |\tilde{S}_1^+|^2 / |\tilde{S}_T^+|}.$$

Thus, for Term ② and $\epsilon = \frac{2\delta}{5|\mu_+ - \mu_-|}$, we have the following bound:

$$\mathbb{P}\left(\underbrace{\frac{1}{2} |\mu_+ - \mu_-| \left|\frac{\sum_{X_i \in \tilde{S}_T^+} I_i^+}{|\tilde{S}_1^+|} - \tilde{A}_T^+ \frac{|\tilde{S}_T^+|}{|\tilde{S}_1^+|}\right|}_{\text{Term ②}} > \frac{\delta}{5}\right) \leq 2e^{-\frac{8\delta^2 |\tilde{S}_1^+|^2}{25(\mu_+ - \mu_-)^2 |\tilde{S}_T^+|}}.$$

When $X_i \in \tilde{S}_1^-$, we can obtain the following two inequality for head and tail data, respectively:

$$\mathbb{P}\left(\left|\frac{\sum_{X_i \in \tilde{S}_H^-} I_i^-}{|\tilde{S}_1^-|} - \tilde{A}_H^- \frac{|\tilde{S}_H^-|}{|\tilde{S}_1^-|}\right| > \epsilon\right) \leq 2e^{-2\epsilon^2 |\tilde{S}_1^-|^2 / |\tilde{S}_H^-|},$$

$$\mathbb{P}\left(\left|\frac{\sum_{X_i \in \tilde{S}_T^-} I_i^-}{|\tilde{S}_1^-|} - \tilde{A}_T^- \frac{|\tilde{S}_T^-|}{|\tilde{S}_1^-|}\right| > \epsilon\right) \leq 2e^{-2\epsilon^2 |\tilde{S}_1^-|^2 / |\tilde{S}_T^-|}.$$

Thus, for Term ③, ④ and $\epsilon = \frac{2\delta}{5|\mu_+ - \mu_-|}$, we have the following bounds:

$$\mathbb{P}\left(\underbrace{\frac{1}{2} |\mu_+ - \mu_-| \left|\frac{\sum_{X_i \in \tilde{S}_H^-} I_i^-}{|\tilde{S}_1^-|} - \tilde{A}_H^- \frac{|\tilde{S}_H^-|}{|\tilde{S}_1^-|}\right|}_{\text{Term ③}} > \frac{\delta}{5}\right) \leq 2e^{-\frac{8\delta^2 |\tilde{S}_1^-|^2}{25(\mu_+ - \mu_-)^2 |\tilde{S}_H^-|}},$$

$$\mathbb{P}\left(\underbrace{\frac{1}{2} |\mu_+ - \mu_-| \left|\frac{\sum_{X_i \in \tilde{S}_T^-} I_i^-}{|\tilde{S}_1^-|} - \tilde{A}_T^- \frac{|\tilde{S}_T^-|}{|\tilde{S}_1^-|}\right|}_{\text{Term ④}} > \frac{\delta}{5}\right) \leq 2e^{-\frac{8\delta^2 |\tilde{S}_1^-|^2}{25(\mu_+ - \mu_-)^2 |\tilde{S}_T^-|}}.$$

Note that

$$\left(\sum_{X_i \in \tilde{S}_1^+} \frac{Z_i^+}{|\tilde{S}_1^+|} + \sum_{X_i \in \tilde{S}_1^-} \frac{Z_i^-}{|\tilde{S}_1^-|}\right) \sim \mathcal{N}\left(\mu_+ + \mu_-, ((|\tilde{S}_1^+| + |\tilde{S}_1^-|)\sigma^2 / (|\tilde{S}_1^+| |\tilde{S}_1^-|))\right),$$

as for Term ⑤, with the standard Gaussian concentration property, we have:

$$\mathbb{P}(\text{Term ⑤} > \epsilon) \leq 2e^{-\frac{\epsilon^2 (|\tilde{S}_1^+| |\tilde{S}_1^-|)}{2\sigma^2 (|\tilde{S}_1^+| + |\tilde{S}_1^-|)}},$$

which is equivalent to:

$$\mathbb{P}(\text{Term ⑤} > \frac{2\delta}{5}) \leq 2e^{-\frac{2\delta^2 (|\tilde{S}_1^+| |\tilde{S}_1^-|)}{25\sigma^2 (\mu_+ - \mu_-)^2 (|\tilde{S}_1^+| + |\tilde{S}_1^-|)}}.$$

Thus, with probability p , we have:

$$\frac{1}{2} |2\tilde{\theta} - (\mu_+ + \mu_-) - \text{Bias}| \leq 5 \cdot \frac{\delta}{5} = \delta,$$

where:

$$\begin{aligned} p &:= 1 - \sum_{i \in [5]} \mathbb{P}(\text{Term } \textcircled{i} > \frac{2\delta}{5}) \\ &= 1 - 2e^{-\frac{8\delta^2 |\tilde{S}_1^+|^2}{25(\mu_+ - \mu_-)^2 |\tilde{S}_H^+|}} - 2e^{-\frac{8\delta^2 |\tilde{S}_1^+|^2}{25(\mu_+ - \mu_-)^2 |\tilde{S}_T^+|}} - 2e^{-\frac{8\delta^2 |\tilde{S}_1^-|^2}{25(\mu_+ - \mu_-)^2 |\tilde{S}_H^-|}} \\ &\quad - 2e^{-\frac{8\delta^2 |\tilde{S}_1^-|^2}{25(\mu_+ - \mu_-)^2 |\tilde{S}_T^-|}} - 2e^{-\frac{2\delta^2 (|\tilde{S}_1^+| |\tilde{S}_1^-|)}{25\sigma^2 (\mu_+ - \mu_-)^2 (|\tilde{S}_1^+| + |\tilde{S}_1^-|)}}. \end{aligned}$$

Further simplification: Now that we have with probability at least p :

$$|2\tilde{\theta} - (\mu_+ + \mu_-) - 2\text{Bias}| \leq \delta \iff \text{Bias} - \delta \leq |\tilde{\theta} - \theta^*| \leq \text{Bias} + \delta.$$

The Bias term could be further simplified as:

$$\begin{aligned} \text{Bias} &= (\mu_- - \mu_+) \left(-\frac{\widetilde{A}_H^+ |\widetilde{S}_H^+| + \widetilde{A}_T^+ |\widetilde{S}_T^+|}{|\widetilde{S}_T^+|} + \frac{\widetilde{A}_H^- |\widetilde{S}_H^-| + \widetilde{A}_T^- |\widetilde{S}_T^-|}{|\widetilde{S}_T^-|} \right) \\ &= (\mu_- - \mu_+) \left(-\frac{(1 - \rho_H^+) |\widetilde{S}_H^+| + (1 - \rho_T^+) |\widetilde{S}_T^+|}{|\widetilde{S}_T^+|} + \frac{(1 - \rho_H^-) |\widetilde{S}_H^-| + (1 - \rho_T^-) |\widetilde{S}_T^-|}{|\widetilde{S}_T^-|} \right) \\ &= \frac{\mu_- - \mu_+}{2} \cdot \left(\frac{\rho_H^+ |\widetilde{S}_H^+| + \rho_T^+ |\widetilde{S}_T^+|}{|\widetilde{S}_H^+| + |\widetilde{S}_T^+|} - \frac{\rho_H^- |\widetilde{S}_H^-| + \rho_T^- |\widetilde{S}_T^-|}{|\widetilde{S}_H^-| + |\widetilde{S}_T^-|} \right) \quad (\text{Due to } |\widetilde{S}_T^\pm| = |\widetilde{S}_H^\pm| + |\widetilde{S}_T^\pm|). \end{aligned}$$

□

B.3 Proof of Lemma A.5

Proof. Note that:

$$\begin{aligned} \text{Err}_{X_H^+}(f) &= \frac{\mathbb{P}(\mathcal{N}(0, 1) < \frac{\theta - \mu_+}{\sigma}, \mathcal{N}(0, 1) \geq -\eta)}{1 - \Phi(-\eta)}, & \text{Err}_{X_T^+}(f) &= \frac{\mathbb{P}(\mathcal{N}(0, 1) < \frac{\theta - \mu_+}{\sigma}, \mathcal{N}(0, 1) < -\eta)}{\Phi(-\eta)}. \\ \text{Err}_{X_H^-}(f) &= \frac{\mathbb{P}(\mathcal{N}(0, 1) > \frac{\theta - \mu_-}{\sigma}, \mathcal{N}(0, 1) \leq \eta)}{1 - \Phi(-\eta)}, & \text{Err}_{X_T^-}(f) &= \frac{\mathbb{P}(\mathcal{N}(0, 1) > \frac{\theta - \mu_-}{\sigma}, \mathcal{N}(0, 1) > \eta)}{\Phi(-\eta)}. \end{aligned}$$

Thus, denote by $p := \mathbb{P}(Y = +)$, we have:

$$\begin{aligned} \text{Err}_{\widetilde{X}_H^+}(f) &= \mathbb{P}_{(\widetilde{X}_H^+, \widetilde{Y})}(\widetilde{f}(\widetilde{X}_H^+) \neq \widetilde{Y}) \\ &= \mathbb{P}(\widetilde{Y} = +, Y = + | X_H^+) \cdot \mathbb{P}_{(\widetilde{X}_H^+, \widetilde{Y})}((\widetilde{X}_H^+ - \theta)Y < 0) + \mathbb{P}(\widetilde{Y} = +, Y = - | X_H^-) \cdot \mathbb{P}_{(\widetilde{X}_H^+, \widetilde{Y})}((\widetilde{X}_H^+ - \theta)Y > 0) \\ &= p \cdot (1 - \rho_H^+) \cdot \mathbb{P}_{(X_H^+, Y=+)}((X_H^+ - \theta)Y < 0) + (1 - p) \cdot \rho_H^- \cdot \mathbb{P}_{(X_H^-, Y=-)}((X_H^- - \theta)Y > 0) \\ &= p \cdot (1 - \rho_H^+) \cdot \mathbb{P}_{(X_H^+, Y=+)}(X_H^+ < \theta) + (1 - p) \cdot \rho_H^- \cdot \mathbb{P}_{(X_H^-, Y=-)}(X_H^- < \theta) \\ &= p \cdot (1 - \rho_H^+) \cdot \text{Err}_{X_H^+} + (1 - p) \cdot \rho_H^- \cdot (1 - \text{Err}_{X_H^-}). \end{aligned}$$

Similarly, we could derive:

$$\begin{aligned} \text{Err}_{\widetilde{X}_H^-}(f) &= \mathbb{P}_{(\widetilde{X}_H^-, \widetilde{Y})}(\widetilde{f}(\widetilde{X}_H^-) \neq \widetilde{Y}) \\ &= \mathbb{P}(\widetilde{Y} = -, Y = + | X_H^+) \cdot \mathbb{P}_{(\widetilde{X}_H^-, \widetilde{Y})}((\widetilde{X}_H^- - \theta)\widetilde{Y} > 0) + \mathbb{P}(\widetilde{Y} = -, Y = - | X_H^-) \cdot \mathbb{P}_{(\widetilde{X}_H^-, \widetilde{Y})}((\widetilde{X}_H^- - \theta)\widetilde{Y} > 0) \\ &= p \cdot \rho_H^+ \cdot \mathbb{P}_{(X_H^+, Y=+)}((X_H^+ - \theta)Y < 0) + (1 - p) \cdot (1 - \rho_H^-) \cdot \mathbb{P}_{(X_H^-, Y=-)}((X_H^- - \theta)Y > 0) \\ &= p \cdot \rho_H^+ \cdot \mathbb{P}_{(X_H^+, Y=+)}(X_H^+ < \theta) + (1 - p) \cdot (1 - \rho_H^-) \cdot \mathbb{P}_{(X_H^-, Y=-)}(X_H^- < \theta) \\ &= p \cdot \rho_H^+ \cdot \text{Err}_{X_H^+} + (1 - p) \cdot (1 - \rho_H^-) \cdot (1 - \text{Err}_{X_H^-}). \end{aligned}$$

$$\text{Err}_{\widetilde{X}_T^+}(f) = p \cdot (1 - \rho_T^+) \cdot \text{Err}_{X_T^+} + (1 - p) \cdot \rho_T^- \cdot (1 - \text{Err}_{X_T^-}).$$

$$\text{Err}_{\widetilde{X}_T^-}(f) = p \cdot \rho_T^+ \cdot \text{Err}_{X_T^+} + (1 - p) \cdot (1 - \rho_T^-) \cdot (1 - \text{Err}_{X_T^-}).$$

□

B.4 Proof of Theorem A.6

Proof. For balanced clean prior ($p = 0.5$), we have:

$$\text{Err}(f) := (1 - \Phi(-\eta)) \cdot \left(\text{Err}_{X_H^+}(f) + \text{Err}_{X_H^-}(f) \right) + \Phi(-\eta) \cdot \left(\text{Err}_{X_T^+}(f) + \text{Err}_{X_T^-}(f) \right),$$

and

$$\begin{aligned}
\text{RM: } \min_f & \mathbb{P}(\widetilde{X}_H^+) \cdot \text{Err}_{\widetilde{X}_H^+}^{\sim}(f) + \mathbb{P}(\widetilde{X}_H^-) \cdot \text{Err}_{\widetilde{X}_H^-}^{\sim}(f) + \mathbb{P}(\widetilde{X}_T^+) \cdot \text{Err}_{\widetilde{X}_T^+}^{\sim}(f) + \mathbb{P}(\widetilde{X}_T^-) \cdot \text{Err}_{\widetilde{X}_T^-}^{\sim}(f) \\
& = \min_f (1 - \Phi(-\eta)) \cdot \left((1 - \rho_H^+ + \rho_H^-) \cdot \text{Err}_{\widetilde{X}_H^+}^{\sim}(f) + (1 + \rho_H^+ - \rho_H^-) \cdot \text{Err}_{\widetilde{X}_H^-}^{\sim}(f) \right) \\
& \quad + \Phi(-\eta) \cdot \left((1 - \rho_T^+ + \rho_T^-) \cdot \text{Err}_{\widetilde{X}_T^+}^{\sim}(f) + (1 - \rho_T^- + \rho_T^+) \cdot \text{Err}_{\widetilde{X}_T^-}^{\sim}(f) \right).
\end{aligned}$$

Define the noise rate gaps $\rho_H := \rho_H^+ - \rho_H^-$, $\rho_T := \rho_T^+ - \rho_T^-$, and imbalance ratio $r := \frac{1 - \Phi(-\eta)}{\Phi(-\eta)}$, we then have:

$$\begin{aligned}
\text{RM} & \iff \min_f r \cdot \left((1 - \rho_H) \cdot \text{Err}_{\widetilde{X}_H^+}^{\sim}(f) + (1 + \rho_H) \cdot \text{Err}_{\widetilde{X}_H^-}^{\sim}(f) \right) + \left((1 - \rho_T) \cdot \text{Err}_{\widetilde{X}_T^+}^{\sim}(f) + (1 + \rho_T) \cdot \text{Err}_{\widetilde{X}_T^-}^{\sim}(f) \right) \\
& \iff \min_f r \cdot \left((1 - \rho_H) \cdot \left[(1 - \rho_H^+) \cdot \text{Err}_{X_H^+} + \rho_H^- \cdot (1 - \text{Err}_{X_H^-}) \right] + (1 + \rho_H) \cdot \left[\rho_H^+ \cdot \text{Err}_{X_H^+} + (1 - \rho_H^-) \cdot (1 - \text{Err}_{X_H^-}) \right] \right) \\
& \quad + \left((1 - \rho_T) \cdot \left[(1 - \rho_T^+) \cdot \text{Err}_{X_T^+} + \rho_T^- \cdot (1 - \text{Err}_{X_T^-}) \right] + (1 + \rho_T) \cdot \left[\rho_T^+ \cdot \text{Err}_{X_T^+} + (1 - \rho_T^-) \cdot (1 - \text{Err}_{X_T^-}) \right] \right) \\
& \iff \min_f r \cdot \left(\left[(1 - \rho_H^+) \cdot \text{Err}_{X_H^+} + \rho_H^- \cdot (1 - \text{Err}_{X_H^-}) \right] + \left[\rho_H^+ \cdot \text{Err}_{X_H^+} + (1 - \rho_H^-) \cdot (1 - \text{Err}_{X_H^-}) \right] \right) \\
& \quad + \left(\left[(1 - \rho_T^+) \cdot \text{Err}_{X_T^+} + \rho_T^- \cdot (1 - \text{Err}_{X_T^-}) \right] + \left[\rho_T^+ \cdot \text{Err}_{X_T^+} + (1 - \rho_T^-) \cdot (1 - \text{Err}_{X_T^-}) \right] \right) \\
& \quad - r \cdot \rho_H \cdot \left(\left[(1 - \rho_H^+) \cdot \text{Err}_{X_H^+} + \rho_H^- \cdot (1 - \text{Err}_{X_H^-}) - \rho_H^+ \cdot \text{Err}_{X_H^+} - (1 - \rho_H^-) \cdot (1 - \text{Err}_{X_H^-}) \right] \right) \\
& \quad - \rho_T \cdot \left[(1 - \rho_T^+) \cdot \text{Err}_{X_T^+} + \rho_T^- \cdot (1 - \text{Err}_{X_T^-}) - \rho_T^+ \cdot \text{Err}_{X_T^+} - (1 - \rho_T^-) \cdot (1 - \text{Err}_{X_T^-}) \right] \\
& \iff \min_f r \cdot \left(\text{Err}_{X_H^+} + \text{Err}_{X_H^-} \right) + \left(\text{Err}_{X_T^+} + \text{Err}_{X_T^-} \right) \\
& \quad - r \cdot \rho_H \cdot \left(\left[(1 - 2\rho_H^+) \cdot \text{Err}_{X_H^+} - (1 - 2\rho_H^-) \cdot (1 - \text{Err}_{X_H^-}) \right] \right) \\
& \quad - \rho_T \cdot \left[(1 - 2\rho_T^+) \cdot \text{Err}_{X_T^+} - (1 - 2\rho_T^-) \cdot (1 - \text{Err}_{X_T^-}) \right] \\
& \iff \min_f \text{Err}(f) - r \cdot \rho_H \cdot \left(\left[(1 - 2\rho_H^+) \cdot \text{Err}_{X_H^+} - (1 - 2\rho_H^-) \cdot (1 - \text{Err}_{X_H^-}) \right] \right) \\
& \quad - \rho_T \cdot \left[(1 - 2\rho_T^+) \cdot \text{Err}_{X_T^+} - (1 - 2\rho_T^-) \cdot (1 - \text{Err}_{X_T^-}) \right]. \tag{4}
\end{aligned}$$

To achieve relatively fair performances between \widetilde{X}_T^+ and \widetilde{X}_T^- , i.e., the performance gap between $\text{Err}_{\widetilde{X}_T^+}^{\sim}(f)$ and $\text{Err}_{\widetilde{X}_T^-}^{\sim}(f)$ is supposed to be small. Note that:

$$\begin{aligned}
& \text{Err}_{\widetilde{X}_T^+}^{\sim}(f) - \text{Err}_{\widetilde{X}_T^-}^{\sim}(f) \\
& = \left[p \cdot (1 - \rho_T^+) \cdot \text{Err}_{X_T^+} + (1 - p) \cdot \rho_T^- \cdot (1 - \text{Err}_{X_T^-}) \right] - \left[p \cdot \rho_T^+ \cdot \text{Err}_{X_T^+} + (1 - p) \cdot (1 - \rho_T^-) \cdot (1 - \text{Err}_{X_T^-}) \right] \\
& = \frac{1}{2} \cdot \left[(1 - 2\rho_T^+) \cdot \text{Err}_{X_T^+} - (1 - 2\rho_T^-) \cdot (1 - \text{Err}_{X_T^-}) \right].
\end{aligned}$$

Similarly, for the two head sub-populations, we could derive that:

$$\begin{aligned}
& \text{Err}_{\widetilde{X}_H^+}^{\sim}(f) - \text{Err}_{\widetilde{X}_H^-}^{\sim}(f) \\
& = \left[p \cdot (1 - \rho_H^+) \cdot \text{Err}_{X_H^+} + (1 - p) \cdot \rho_H^- \cdot (1 - \text{Err}_{X_H^-}) \right] - \left[p \cdot \rho_H^+ \cdot \text{Err}_{X_H^+} + (1 - p) \cdot (1 - \rho_H^-) \cdot (1 - \text{Err}_{X_H^-}) \right] \\
& = \frac{1}{2} \cdot \left[(1 - 2\rho_H^+) \cdot \text{Err}_{X_H^+} - (1 - 2\rho_H^-) \cdot (1 - \text{Err}_{X_H^-}) \right].
\end{aligned}$$

Thus, by incorporating the above two performance gaps into Eqn. (4), the RM has its equivalent form as below:

$$\begin{aligned} \text{RM} &\iff \min_f \text{Err}(f) - r \cdot \rho_H \cdot \left(\left[(1 - 2\rho_H^+) \cdot \text{Err}_{X_H^+} - (1 - 2\rho_H^-) \cdot (1 - \text{Err}_{X_H^-}) \right] \right) \\ &\quad - \rho_T \cdot \left[(1 - 2\rho_T^+) \cdot \text{Err}_{X_T^+} - (1 - 2\rho_T^-) \cdot (1 - \text{Err}_{X_T^-}) \right] \\ &\iff \min_f \text{Err}(f) - 2r \cdot \rho_H \cdot \left(\text{Err}_{X_H^+}^{\sim}(f) - \text{Err}_{X_H^-}^{\sim}(f) \right) - \rho_T \cdot \left(\text{Err}_{X_T^+}^{\sim}(f) - \text{Err}_{X_T^-}^{\sim}(f) \right). \end{aligned}$$

□

C Additional Experiment Results and Details

C.1 Influences of sub-populations on test data

Influences on Class-Level Test Accuracy When removing all samples from the sub-population \mathcal{G}_i during the whole training procedure, remember that we defined the (class-level) test accuracy changes as:

$$\text{Acc}_c(\mathcal{A}, \tilde{S}, i, j) := \mathbb{P}_{\substack{f \leftarrow \mathcal{A}(\tilde{S}) \\ (X', Y' = j)}} (f(X') = Y') - \mathbb{P}_{\substack{f \leftarrow \mathcal{A}(\tilde{S} \setminus i) \\ (X', Y' = j)}} (f(X') = Y'),$$

where $(X', Y' = j)$ indicates the test data distribution given the clean label is j . In Figure 8, the x -axis denotes the loss function for training, and the y -axis visualized the distribution of $\{\text{Acc}_c(\mathcal{A}, \tilde{S}, i, j)\}_{j \in [10]}$ (above the dashed line) and $\{\text{Acc}_c(\mathcal{A}, \tilde{S}, i, j)\}_{j \in [10]}$ (below the dashed line) for several long-tailed sub-populations ($i = 52, 37, 75, 19, 81, 36, 91, 63, 70, 55, 67, 41, 98, 40, 61, 87, 71$) under each robust method. The blue zone shows the 25-th percentile (Q_1) and 75-th percentile (Q_3) accuracy changes, and the orange line indicates the median value. Accuracy changes that are drawn as circles are viewed as outliers. Note that all sub-figures have the same limits for y -axis, Observation 3.1 holds for more tail sub-populations under class-level test accuracy as well.

Influences on Population-Level Test Accuracy When removing all samples from the sub-population $\mathcal{G}^{(i)}$ during the whole training procedure, remember the (population-level) test accuracy changes are defined as:

$$\text{Acc}_p(\mathcal{A}, \tilde{S}, i, j) := \mathbb{P}_{\substack{f \leftarrow \mathcal{A}(\tilde{S}) \\ (X', Y', G = j)}} (f(X') = Y') - \mathbb{P}_{\substack{f \leftarrow \mathcal{A}(\tilde{S} \setminus i) \\ (X', Y', G = j)}} (f(X') = Y'),$$

where $(X', Y', G = j)$ indicates the test data distribution given that the samples are from the j -th population. In Figure 9, we repeat the previous step while visualize the distribution of $\{\text{Acc}_p(\mathcal{A}, \tilde{S}, i, j)\}_{j \in [100]}$ (Above the dashed line) and $\{\text{Acc}_p(\mathcal{A}, \tilde{S}, i, j)\}_{j \in [100]}$ (Below the dashed line). Similarly, by referring to the wide range of box plotted distributions, Observation 3.1 holds for more tail sub-populations as well. Besides, the variance and the extremers of the changes in the test accuracy are much larger in the view of sub-populations.

Influences on Sample-Level Prediction Confidence Remember that we characterize the influence of a sub-population on a test sample as:

$$\text{Infl}(\mathcal{A}, \tilde{S}, i, j) := \mathbb{P}_{f \leftarrow \mathcal{A}(\tilde{S})} (f(x'_j) = y'_j) - \mathbb{P}_{f \leftarrow \mathcal{A}(\tilde{S} \setminus i)} (f(x'_j) = y'_j),$$

where in the above two quantities, $f \leftarrow \mathcal{A}(\tilde{S})$ denotes that the classifier f is trained from the whole noisy training dataset \tilde{S} via Algorithm \mathcal{A} , $f \leftarrow \mathcal{A}(\tilde{S} \setminus i)$ means f got trained on \tilde{S} without samples in the sub-population $\mathcal{G}^{(i)}$. And $\text{Infl}(\mathcal{A}, \tilde{S}, i, j)$ quantifies the influence of a certain sub-population on specific test data. As shown in Figure 10, we visualize $\text{Infl}(\mathcal{A}, \tilde{S}, i, j)$ (1st row) and $\text{Infl}(\mathcal{A}, \tilde{S}, i, j)$ (2nd row), where $j \in [10000]$ means 10K test samples. With the presence of label noise, Observations 3.2 holds for more tail sub-population as well.

C.2 Experiment Details on CIFAR Datasets

Hyper-Parameter Settings For each baseline method, we adopt mini-batch size 128, optimizer SGD, initial learning rate 0.1, momentum 0.9, weight decay 0.0005, number of epochs 200. As for the learning rate scheduler, we followed [4] and chose a linear warm-up of learning rate [6] in the first 5 epochs, then decay 0.01 after the 160-th epoch and 180-th epoch. Standard data augmentation is applied to each synthetic CIFAR dataset. We did not make use of any advanced re-sampling strategies or data augmentation techniques. All experiments run on a cluster of Nvidia RTX A5000 GPUs.

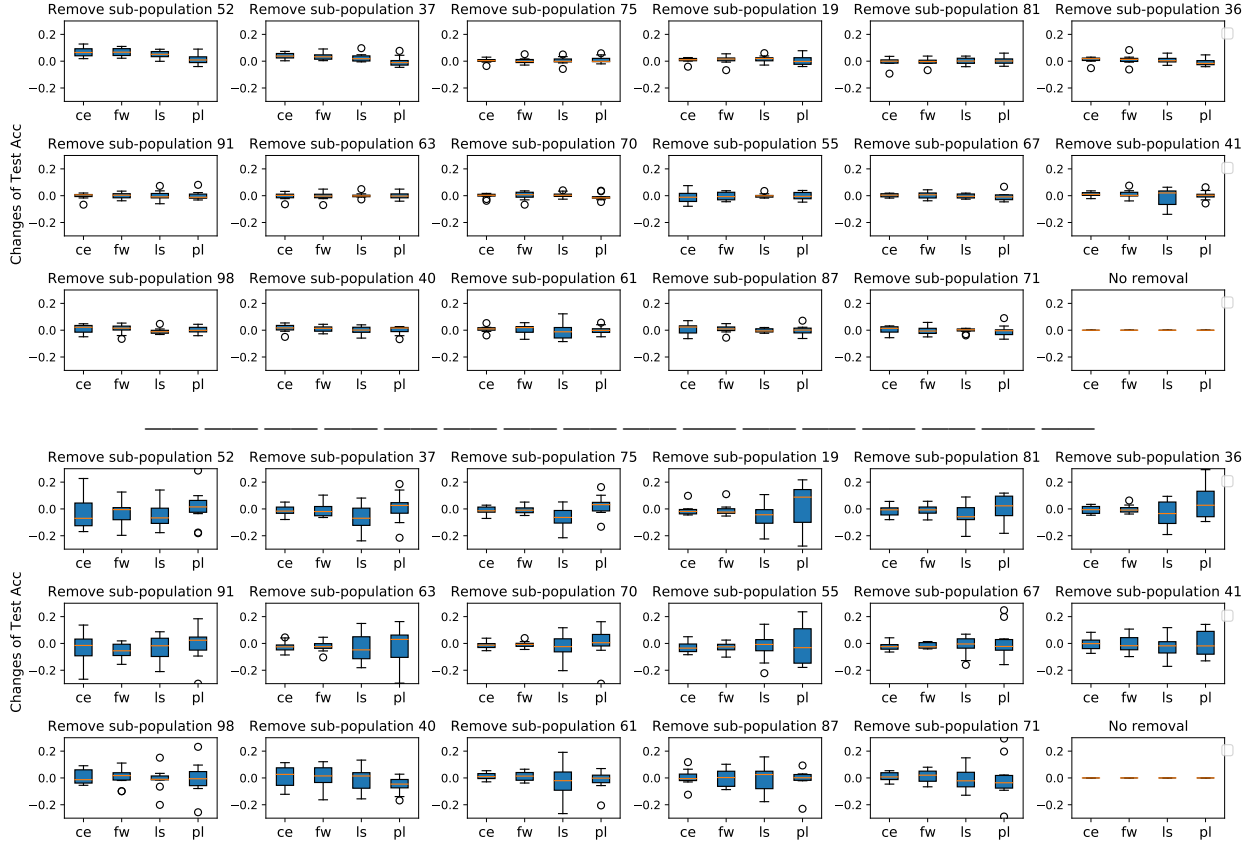


Figure 8: (Completed version) Box plot of the class-level test accuracy changes when removing all samples of a selected long-tailed sub-population during the training w.r.t. 4 methods. (Above the dashed line: trained on clean labels; below the dashed line: trained on noisy labels.)

The Value of λ in FR (KNN) We tuned the performance of FR (KNN) w.r.t. a set $\{0.0, 0.1, 0.2, 0.4, 0.6, 0.8, 1.0, 2.0\}$, where $\lambda = 0.0$ indicates the training of baseline methods without **FR**. Regarding the reported results in the main paper: for all methods w.r.t. CIFAR-100 dataset, we set $\lambda = 0.1$ since calculating the accuracy of tail sub-populations may be unstable. As for methods on CIFAR-10 Imb noise, we set $\lambda = 1.0$ for CE loss, NLS, Focal loss and Peer Loss. One exception is that LS requires a relative small λ , i.e., $\lambda = 0.4$. Also, we observe that for Imb noise, a larger λ could be more beneficial for CE loss and Logit-adj loss under a higher noise regime. For methods on CIFAR-10 Sym noise, the λ selection for LS, NLS, PeerLoss remains the same as that in the Imb setting. For CE and Focal loss, a larger λ (i.e., $\lambda = 2.0$) could be more beneficial. While Logit-adj prefers a smaller λ (i.e., $\lambda = 0.5$).

The Value of λ in FR (G2) Since there are only two sub-populations considered, the experiment results on CIFAR-100 would be more stable than FR (KNN), hence a larger λ could be utilized. For CE loss, NLS and Focal loss, we adopt $\lambda = 1.0$ for all CIFAR-10 experiments and $\lambda = 2.0$ for all CIFAR-100 experiments. For LS, we set $\lambda = 0.4$ for all experiments, except for the extreme case (CIFAR-100 with large noise $\rho = 0.5$), where we decide on a larger λ (0.8). As for PeerLoss, we have to set a relatively small λ (i.e., $\lambda = 0.8$) for CIFAR-10 experiments and an even smaller one ($\lambda = 0.2$) on CIFAR-100 due to the scale of its loss. And we set $\lambda = 1.0$ for Logit-adj under all settings. We do observe better results when adopting varied λ under each setting, but fixing the λ for reporting under a specific dataset tends to be more convenient and practical.

C.3 Experiment Details on Clothing1M Dataset

We adopt the same baselines as reported in CIFAR experiments for Clothing1M. All methods use the pre-trained ResNet50, optimizer SGD, momentum 0.9, and weight decay $1e-3$. The initial learning rate is 0.01, then it decays

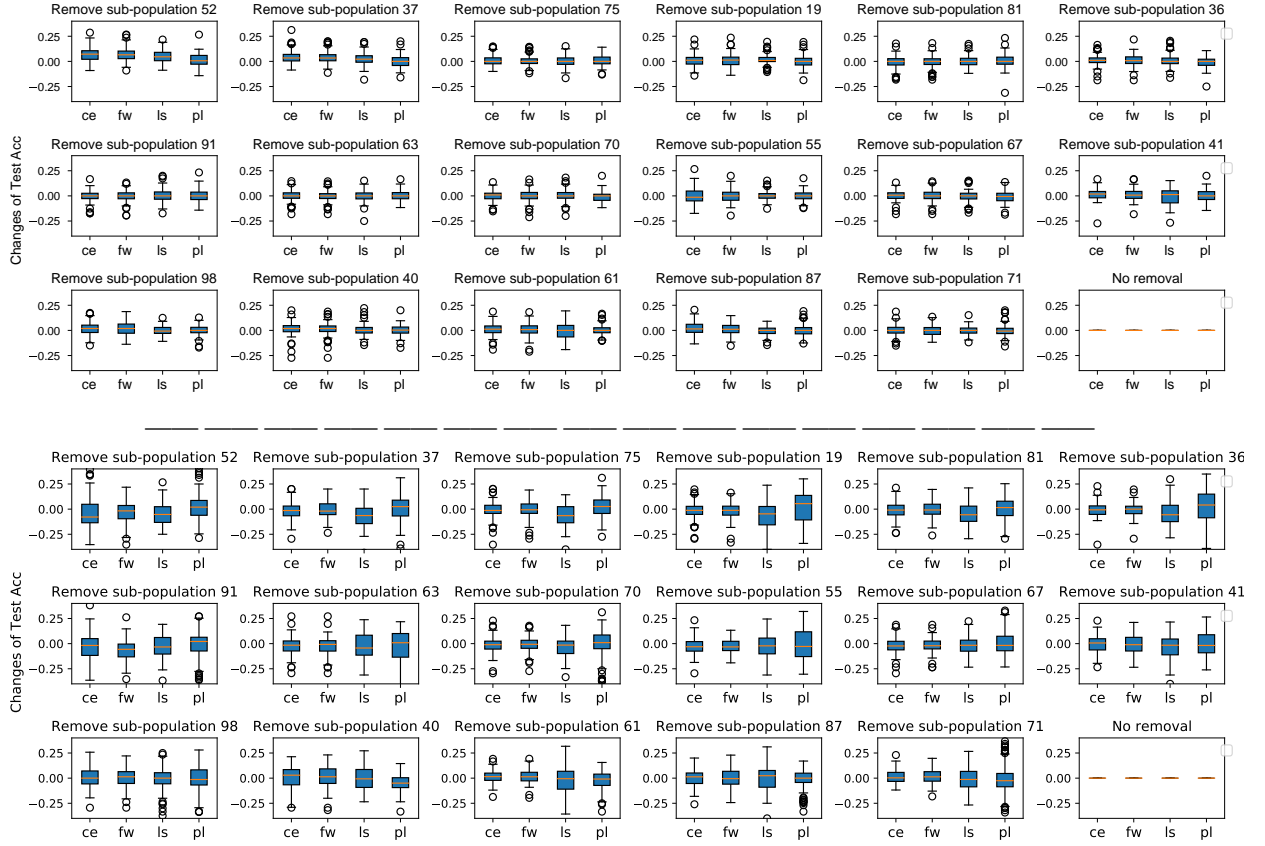


Figure 9: (Complete version) Box plot of the population-level test accuracy changes when removing all samples of a selected long-tailed sub-population during the training w.r.t. 4 methods. (Above the dashed line: trained on clean labels; Below the dashed line: trained on noisy labels.)

0.1 for every 30 epochs so there are 120 epochs in all. Negative Label Smoothing (NLS) [56] resumes the last epoch training of CE, and proceeds to train with NLS for another 40 epochs (learning rate $1e-7$).

C.4 Influences of head sub-populations on test data

Table 5 briefly introduces the influences of head populations (> 500 samples) on the overall test accuracy. Clearly, the mentioned 5 head populations have different impacts: with the presence of label noise, Pop-06 becomes harmful while Pop-02 and Pop-04 remain helpful.

Table 5: Influences of head populations on the overall test accuracy.

Clean	Remove Pop-02	Remove Pop-04	Remove Pop-03	Remove Pop-06	Remove Pop-00
Test Acc	-4.06	-3.09	-0.96	-0.15	+0.29
Noisy $\rho = 0.2$	Remove Pop-02	Remove Pop-04	Remove Pop-03	Remove Pop-06	Remove Pop-00
Test Acc	-3.75	-4.80	-3.79	+0.62	+0.18

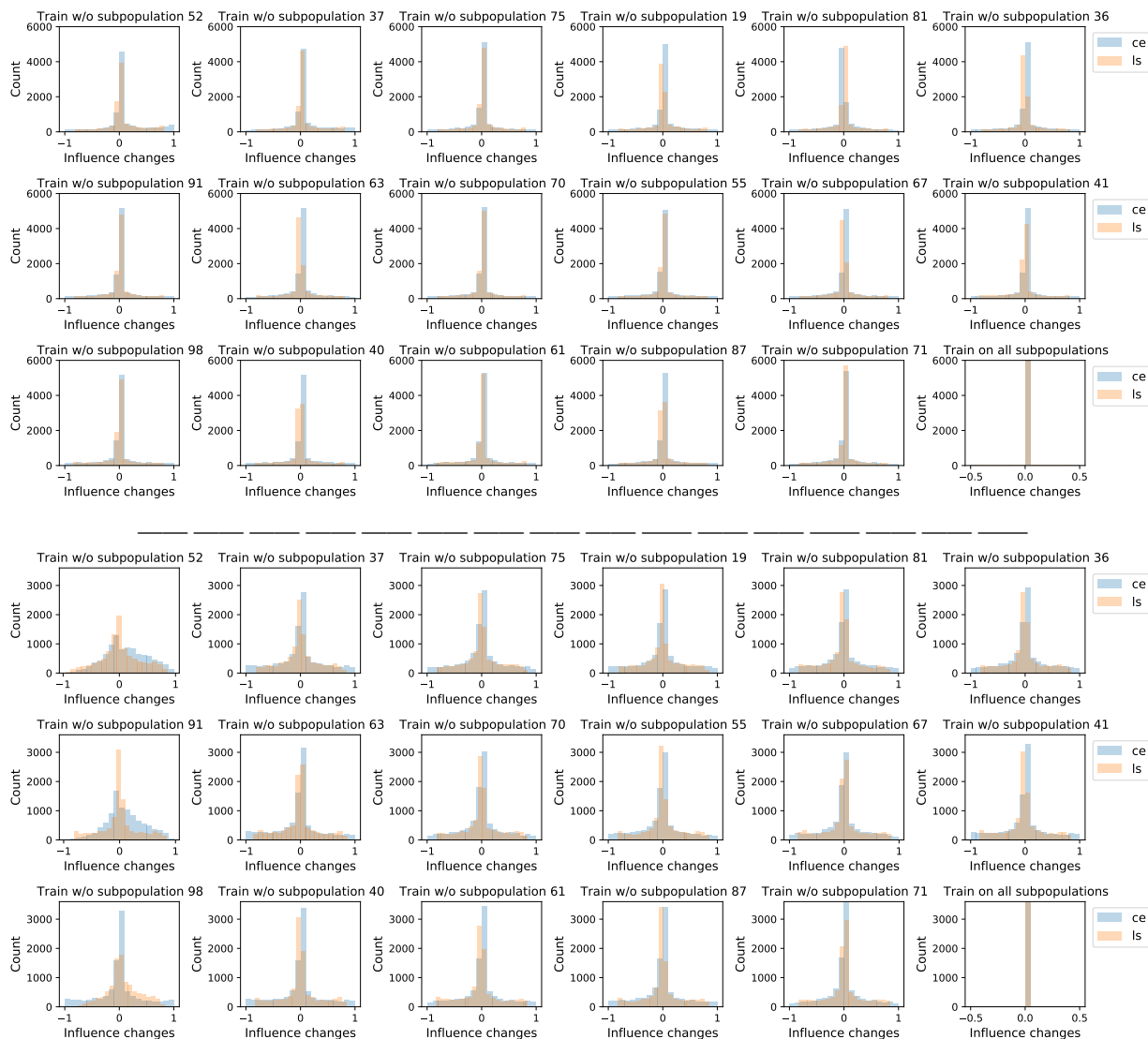


Figure 10: (Complete version) Distribution plot w.r.t. the changes of model confidence on the test data samples using CE loss and label smoothing (Above the dashed line: trained on clean labels; Below the dashed line: trained on noisy labels).